Non-contextual inequalities and dimensionality

Johan Ahrens

ISBN 978-91-7649-197-3
Printer: Holmbergs, Malmö Sweden, 2015
Distributor: Department of Physics, Stockholm University

Abstract

This PhD-thesis is based on the five experiments I have performed during my time as a PhD-student. Three experiments are implementations of non-contextual inequalities and two are implementations of witness functions for classical- and quantum dimensions of sets of states.

A dimension witness is an operator function that produce a value when applied to a set of states. This value has different upper bounds depending on the dimension of the set of states and also depending on if the states are classical or quantum. Therefore a dimension witness can only give a lower bound on the dimension of the set of states.

The first dimension witness is based on the CHSH-inequality and has the ability of discriminating between classical and quantum sets of states of two and three dimensions, it can also indicate if a set of states must be of dimension four or higher.

The second dimension witness is based on a set theoretical representation of the possible combinations of states and measurements and grows with the dimension of the set of states you want to be able to identify, on the other hand there is a formula for expanding it to arbitrary dimension.

Non-contextual hidden variable models is a family of hidden variable models which include local hidden variable models, so in a sence non-contextual inequalities are a generalisation of Bell-inequalities. The experiments presented in this thesis all use single particle quantum systems.

The first experiment is a violation of the KCBS-inequality, this is the simplest correlation inequality which is violated by quantum mechanics.

The second experiment is a violation of the Wright-inequality which is the simplest inequality violated by quantum mechanics, it contains only projectors and not correlations.

The final experiment of the thesis is an implementation of a Hardy-like equality for non-contextuality, this means that the operators in the KCBS-inequality have been rotated so that one term in the sum will be zero for all non-contextual hidden variable models and we get a contradiction since quantum mechanics gives a non-zero value for all terms.

Sammanfattning på Svenska

Denna doktorsavhandling är baserad på fem experiment jag har utfört under min tid som doktorand. Tre experiment är realiseringar av icke-kontextuella olikheter och de två övriga är realiseringar av vittnesfunktioner för klassiska och kvantmekaniska dimensioner hos en uppsättning tillstånd.

Ett dimensionsvittne är en funktion som tar en uppsättning tillstånd och producerar ett värde. Detta värde har olika övre gränser beroende på dimensionen hos uppsättningen tillstånd och beror även på om tillstånden är klassiska eller kvantmekaniska. På grund av detta kan ett dimensionsvittne endast ge en undre uppskattning på dimensionen hos en uppsättning tillstånd.

Det första dimensionsvittnet är baserat på CHSH-olikheten och kan urskilja mellan klassiska och kvantmekaniska tillstånd av två och tre dimensioner, det kan även avgöra ifall uppsättningen av tillstånd har dimension fyra eller högre.

Det andra dimensionsvittnet är baserat på en sannolikhetsteoretisk representation av möjliga kombinationer av tillstånd och mätningar. Detta vittne växer med antalet dimensioner som skall kunna urskiljas, å andra sidan finns det en formel för hur man kan expandera vittnet till godtycklig dimension.

Icke-kontextuella gömda-variabel-teorier är en familj av gömda-variabel-teorier som innefattar lokala gömda-variabel-teorier, så i en bemärkelse är icke-kontextuella olikheter en generalisering av Bell-olikheter. Experimenten i denna avhandling använder sig alla av en-partikel-kvantsystem.

Det första experimentet är en brytning av KCBS-olikheten, det är den enklaste olikheten baserad på korrelationer som kan brytas av kvantmekanik.

Det andra experimentet är en brytning av Wright-olikheten som är den enklaste olikheten som kan brytas av kvantmekanik, den innehåller endast projektorer inga korrelationer.

Det sista experimentet i avhandlingen är en realisering av en Hardy-lik olikhet för icke-kontextualitet. Detta betyder att operatorerna i KCBS-olikheten har roterats så att en term i summan är identiskt noll för alla icke-kontextuella gömda-variabel-teorier och vi får en motsägelse då kvantmekaniken ger ett noll-skiljt värde för alla termer.

List of Papers

The following papers, referred to in the text by their Roman numerals, are included in this thesis.

PAPER I: **Experimental tests of classical and quantum dimensionality**
J. Ahrens, P. Badziąg, M. Pawłowski, M. Żukowski,
and M. Bourennane,
Phys. Rev. Lett., **112**, 140401 (2014).

PAPER II: **Experimental device-independent tests of classical and quantum dimensions**
J. Ahrens, P. Badziąg, A. Cabello, and M. Bourennane,
Nature physics, **8**, 592 (2012).

PAPER III: **Two fundamental experimental tests of non-classicality with qutrits**
J. Ahrens, E. Amselem, M. Bourennane, and A. Cabello,
Sci. Rep, **3**, 02170 (2013).

PAPER IV: **Experimental observation of Hardy-like quantum contextuality**
B. Marques, J. Ahrens, M. Nawareg, A. Cabello,
and M. Bourennane,
Phys. Rev. Lett., **113**, 250403 (2014).

Author's contribution

PAPER I: The experimental setup is based on the setup designed for paper III. I built the setup, made the measurements, and analysed the data. The paper was written by all the co-authors.

PAPER II: The experimental setup is based on the setup designed for paper III. I built the setup, made the measurements, and analysed the data. The paper was written by all the co-authors.

PAPER III: The design of the time encoding scheme and the experimental setup was done by Elias Amselem and me with equal contributions. We built the setup and made the measurements and data analysis together. The paper was written by all the co-authors.

PAPER IV: I did initial investigation for the design of the experimental setup. The design was finished by Breno Marques.

Contents

Abbreviations

APD	Avalanche Photo Detector
BB84	Bennett, Brassard 1984
CHSH	Clauser, Horne, Shimony, and Holt
CMOS	Complementary Metal Oxide Semiconductor
EPR	Einstein, Podolsky, and Rosen
HVT	Hidden Variable Teory
HWP	Half Wave Plate
KCBS	Klyachko, Can, Biniocioğlu, and Shumovsky
LHVT	Local Hidden Variable Teory
NCHVT	Non-Contextual Hidden Variable Teory
OD	Optical Density (filter)
PBS	Polarizing Beam Splitter
QWP	Quarter Wave Plate

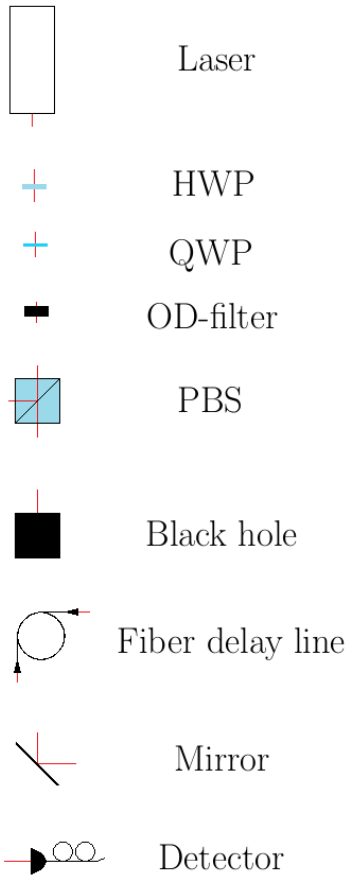

Figure 1: The optical components used in the experiments.

Part I

Background

1. Introduction

This thesis will describe the experiments (detailed in papers I-IV) I have been part of conducting as a PhD-student in the Quantum Information and Quantum Optics group at Fysikum at Stockholm University. We will start with a brief background where the key concepts will be introduced[1]. Topics that are good to have in mind when reading the thesis include qubits and their higher dimensional derivatives, dimensions of physical entities, and the implications of contextuality, locality, and realism. I will also, mostly as a curiosity, show some connections between graphs and non-contextual inequalities.

[1]N.B. this is not to be considered a textbook on the subject, a background in physics and familiarity of quantum mechanics is assumed.

1.1 Quantum state preparation

When you do calculations in quantum mechanics you usually want to answer something like: "if a spin-half particle in the state $|\psi\rangle = \frac{1}{\sqrt{2}}(|\uparrow\rangle_z + e^{i\varphi}|\downarrow\rangle_z)$ pass through a Stern-Gerlach apparatus aligned in the z-direction, what are the possible measurement outcomes and their corresponding probabilities?". This is quite straight forward and it only takes a line or two to write down the answer. In this thesis however we are discussing experimental quantum mechanics, so how would you do the same thing experimentally? To start with you need a source of spin-half particles and some way of changing the state of the particles in a controlled manner. Depending on the motivation for the experiment and the assumptions made you may need to make sure that you can eject single particles from the source. Say we want to make an 'optical Stern-Gerlach' experiment, this will work well since the photon, even though it is a spin-one particle, only assume the spin states -1 and 1[1]. The spin of the photon is directly related to the polarization of the classical light field which the photon would seem to be a part of. Thus a polarizing beam splitter (PBS) will work as a Stern-Gerlach apparatus, and the convention is that horizontal polarization corresponds to spin 1 and vertical polarization corresponds to spin -1 in the z-basis[2]. An even superposition, with real coefficients, of these spin states gives the x-basis, where spin 1 corresponds to diagonal polarization and spin -1 to anti-diagonal. This means that if we want to align our Stern-Gerlach apparatus in the x-direction all we need to do is rotate it 45 degrees around the direction of propagation. This is a bit cumbersome however and an equivalent action is to put half wave-plates (HWP) before and after the PBS and rotate them by an angle of 22.5 degrees[3] but more of this in the next section.

Now back to the state $|\psi\rangle$, we need a source of photons, in this thesis we will use a laser. The laser emits light with a certain polarization and the first thing to do is to determine which it is. The simplest way to do this is with a PBS, two HWPs, and a quarter wave-plate (QWP)[4]. Next we use wave-plates to rotate the polarization to the polarization corresponding to the state $|\psi\rangle$. The final thing we need to do is attenuate the laser light until we only have one photon at a time.

[1] Photons with helicity zero are called virtual photons and cannot be directly detected.

[2] In this notation the positive y-direction is taken to be the direction of propagation and thus spin 1 in the y-basis corresponds to right circular polarization, and -1 to left circular polarization.

[3] Please see appendix A for the behavior of PBSs and HWPs.

[4] More information in appendix A.

1.2 Measurement

In this section I will describe the idea behind and the implementation of the quantum optical measurement system that has been used in the experiments. We have taken the viewpoint that a measurement can be divided into two parts, first a transformation to the eigenbasis of the observable and then detection of the eigenstates. This approach is especially useful when making sequential measurements since it is a simple task to entangle the different eigenstates with other degrees of freedom of the photon. After which we transform back to the laboratory basis. At this point we can choose to either send the photon to another observable or to detection.

The system will be presented in a box framework. First we have the P-box, state preparation, this is followed by the U-box, unitary transformation to eigenbasis of the observable. Then comes the E-box, entangling eigenstates with other degrees of freedom, the $U^{\dagger}$-box, unitary transformation back to the laboratory basis. Finally we have the D-box, the detection of the photon. The block of U->E->$U^{\dagger}$ can be interpreted as a non-demolishing measurement, and by adding more of these blocks sequential measurements can be done.

1.2.1 Box framework

- **P-box -** The P-box is the first box in the setup used in the experiments presented in this thesis. P stands for preparation and the P-box is where the states needed for alignment of the operators, as well as those needed for testing the inequalities, are prepared. The states are encoded in what will be called the laboratory basis.

- **U-box -** The second box in the setup is the U-box. U stands for unitary transformation of the state from the laboratory basis to the eigenbasis of the observable to be measured.

- **E-box -** The middle box is the E-box. E stands for entangling the eigenstates with some other mode[1] of the state.

- **$U^\dagger$-box -** The fourth box is the $U^\dagger$-box. $U^\dagger$ stands for the inverse unitary transformation, i.e, the transformation back to the laboratory basis.

- **D-box -** The final box is the D-box. D stands for detection and it is where the particle is destroyed in order to get a click in the detector.

These boxes are all clearly implementation technology dependent but the one which might need a bit more looking into is the E-box. To entangle the eigenstates we can choose whichever mode we want for each eigenstate, as long as it is not used for something else. What we mean by entangling here is that we add information to the state so that the different eigenstates are distinguishable, even after further evolvement of the state. Take for instance a qubit encoded in the polarization in a single spatial mode. If you want to measure this qubit you will probably use a phase-plate of some kind to rotate it to the basis you want to measure it in[2]. Then you put a PBS in the beam and detectors to detect the horizontal and the vertical parts, respectively. What you actually do with the PBS is that you entangle the eigenstate "+" with the spatial mode transmitted into by the PBS and the eigenstate "-" with the spatial mode reflected into by the PBS. You have added information to the state specifying that if you find the photon at this point it is this specific eigenstate.

[1] I.e., other than those used for encoding.
[2] This is the U-box by the way.

1.2.2 Sequential measurements

When making sequential measurements the box framework is very convenient to work with, all observables are implemented in the same way and there is a laboratory basis as reference between all observables so there is little room for confusion of how the state is encoded. In the papers presented in this thesis two different systems have been used but for clarity we will start with a third system that might be easier to grasp[1]. In all the systems we start with a P-box, followed by a U-box, then differences will come in the E-box where we entangle the eigenstates with different degrees of freedom.

In the first example, see Fig. (1.1), we entangle the eigenstates with different spatial modes. This leads to the fact that we need two $U^\dagger$-boxes, one in each spatial mode. It also means that we will have two instances of the second operator, one after each $U^\dagger$-box. Each of these will have a U-box, an E-box, and two $U^\dagger$-boxes. Finally we will have four D-boxes, one after each $U^\dagger$-box. These four will represent outcomes "++"[2], "+-", "-+", and "–" which is all the possible combinations we can get from this simple experiment[3]. Since all outcomes are spatially separated the D-boxes need to consist only of detectors and depending on which detector clicks the different outcomes can be inferred.

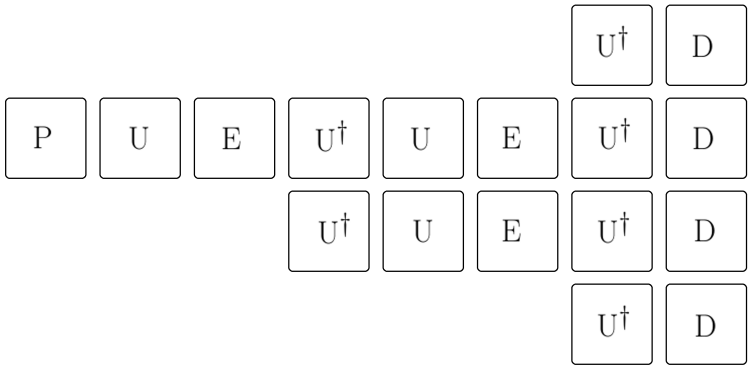

Figure 1.1: In this schematic we have an overview of two sequential measurements where the outcomes are encoded in spatial modes. After the first E-box we need two $U^\dagger$-boxes since we have two different outcomes. Likewise after the second set of E-boxes, we have two $U^\dagger$-boxes each which finally results in four D-boxes. It is noteworthy that each D-box must contain two detectors, since even though we have a two level system we transform back to the laboratory basis.

[1]To keep the complexity as low as possible we consider only two dimensional states and two consecutive measurements.

[2]Reading as; plus for the first observable and plus for the second.

[3]Note that this is the way the Stern-Gerlach experiment is usually presented in introductory textbooks.

In the second example, see Fig. (1.2), the E-box instead entangle the eigenstates with time modes, i.e., separating the eigenstates by a certain amount of time[1]. This system requires a pulsed laser so that the photons will arrive at specific times. The benefit of this system as opposed to the previous, is that we only need one $U^{\dagger}$-box and a single instance of the second operator. We will also need only one D-box, however we will need some kind of synchronization device to distinguish between the different outcomes. The D-box will also in this case be just detectors, which indicates if a photon has been detected, the times at which it can detect a photon will give us the four outcomes "++", "+-", "-+", and "–".

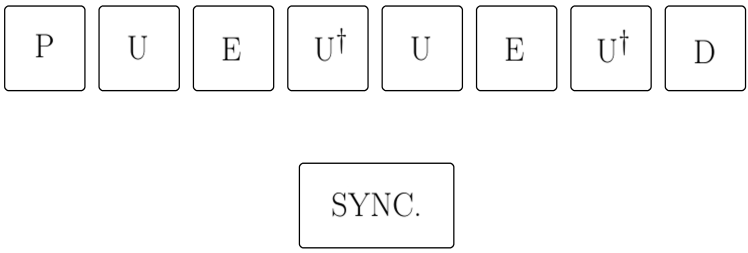

Figure 1.2: In this schematic we have encoded the outcomes in time, so in the E-boxes there is a delay device which separates the two outcomes. Of course the delay has to be different in the two E-boxes, so that we get four well separated times. In addition to the optical setup we also need a synchronization box which synchronizes the detector clicks with the pulsing of the laser, so that we know which detector click belongs to which outcome.

[1]Larger than the coherence time of the photon.

The final example, see Fig. (1.3), comes with three restrictions; first: you are not allowed to use the polarization for encoding your state, second: you can only make two consecutive measurements, and third: the measurements must be dichotomic. The reason for these restrictions is that the first E-box will entangle the eigenstates with polarization modes. Again, it has the benefit of just needing one $U^\dagger$-box and a single instance of the second operator[1]. In addition it does not need any synchronization device to distinguish between outcomes. A drawback however, is that it consumes a lot of detectors since the D-box will have a PBS in each of the modes, and each detector will represent one of the outcomes "++", "+-", "-+", and "–".

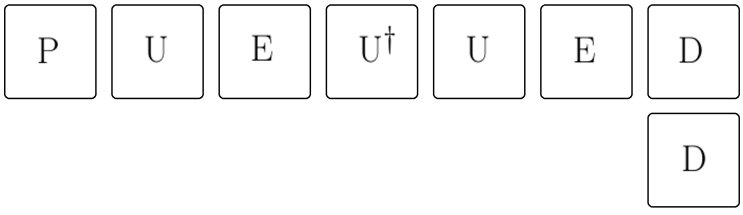

Figure 1.3: In this last schematic the first E-box encodes the outcomes in polarization modes and the second one in spatial modes. This makes for a compact setup without delays and thus without the need of a pulsed source. However, we need PBSs to translate the polarization modes to spatial modes and thus we need four detectors in order to register all of our outcomes.

[1]The simplest implementation of the second operator is to let the E-box entangle the eigenstates with different spatial modes, in this way a detector in each spatial mode will give the outcomes of the second operator. No $U^\dagger$-box is needed since there will only be detection of the photons after the operator.

1.3 Dimensions

As with all words that are used in daily life, most people have an idea of what the word dimension means. This meaning might differ depending on the person and the situation and thus we need to define how we will use the word in this thesis[1]. To start with we note that dimensionality is a property of a set of states not of a single state, it is only when we compare it with other states that we see how much information we need, to fully distinguish it from the rest. This leads us to the definition of classical dimension; the number of distinguishable states in a set, e.g. the two dimensions used in CMOS technology are defined as the ranges 0V - $\frac{1}{3}V_{DD}$[2], corresponding to '0', and $\frac{2}{3}V_{DD}$ - V_{DD}, corresponding to '1'. For a quantum system we are not satisfied with just having distinguishability of the states, we demand that they span a Hilbert space, i.e., the states must be superposable. This is a purely experimental issue since if you have a set of orthonormal state vectors $|i\rangle$ it is easy to write a general state $|\psi\rangle = \frac{1}{\sqrt{\sum \alpha_i \alpha_i^*}} \sum_0^N \alpha_i |i\rangle$, however just because you can make a number of states in the lab does not mean you can easily construct any superposition of them. As an example of a two dimensional quantum system we can take the spin states of photons, if we can prepare spin 1 and spin -1 in the z-basis and then measure in the x-basis we see that both are superpositions of spin 1 and spin -1 in that basis.

[1] It is important with a clear definition of all concepts in physics but especially necessary for words which have a relaxed or different meaning outside of physics.

[2] V_{DD} is the supply voltage.

1.4 Classicality and quantumness

The aim of this thesis is to illustrate different ways of discerning the descrepancy between classical and quantum mechanics.

In macroscopic mechanics, objects have pre-established properties which does not change depending on which measurements (or lack there of) are made. Take for instance a ball and two boxes, now the boxes can contain the ball or be empty. This is fact and will not change unless we add or remove the ball to/from the boxes. Extrapolating this idea to microscopic systems might be intuitive and we call this a classical viewpoint.

According to quantum mechanics however, particles (e.g. photons) do not have pre-established properties in this way. Let the polarisation state of an ensemble of photons correspond to the boxes in the example above, where horizontal polarisation would be the ball in box one, vertical polarisation; the ball in box two and if you would detect both horizontal and vertical polarisation, this would correspond to both boxes being empty. So far it would seem there is no difference between the two examples, but if you were to rotate you measurement apparatus 45 degrees around the axis of propagation the result would be completely different. If the photons were created horizontally then half of the photons would end up in each of the detectors in the new measurement apparatus, the same for vertically created photons. The photons that were created to have equal probability to be horizontal and vertical could be any of the three possible outcomes (depending on how they were created). While the classical viewpoint perhaps was intuitive, this modern viewpoint explain experimental results and successfully predict how the world will behave, giving rise to many technological advancements.

Note that the randomness, or unpredictability, that arises from quantum mechanics is not due to lack of knowledge but is inherent to the system. In contrast, the state of the ball and boxes can seem unpredictable if we are not present when the system is prepared. However, most of us would agree that there is a "true" state of the boxes which is just unknown to us[1].

[1]Think of a small child who is present when the system of ball and boxes is prepared. When asked what a person not present at the preparation would answer about the state, the child (until a certain degree of maturity) would indicate the box with the ball in it, thinking that fact is fact.

1.5 Realism

Since the begining of quantum mechanics there has been a discussion about what the wavefunction really describes and if this description can be considered a complete description of the system at hand.

In 1935 Albert Einstein, Boris Podolsky and Nathan Rosen wrote an article[1] were they argue against quantum mechanics being complete. They make the assumption that the world we live in must have an 'objective reality', and quantum mechanics clearly states that two noncommuting operators cannot be simultaneously determined. They conclude that since there exist some special states, so called EPR-pairs, in which a particle simultaneously can have elements of reality for two noncommuting operators quantum mechanics is incomplete. John Bell wrote, in 1964, an article in which he derives a theorem which states that, using states of the same kind as EPR you can make certain measurements for which quantum mechanics will give a higher expectation value than any local hidden-variable theory[1] (LHVT). These measurements on the right kind of state were made experimentally by Freedman and Clauser in 1972[2]. They used photons from radiative calcium to generate meaurement results which exceeded the 'classical bound' in Bell's theorem and thus gave the first experimental evidence that the world is not governed by local-realism. These results show that there is a fundamental flaw in the classical understanding of the world, and that this flaw is made visible under the assumption of locality.

Another direction was taken by Simon B. Kochen and Ernst Specker in 1967[3], when they considered a larger family of hidden-variable theories (HVT), the non-contextual ones. The idea is basically the same as the one of Bell, you can find a set of measurements for which the expectaion value of quantum mechanics exceed that of any non-contextual hidden-variable theory (NCHVT). The first experimental verification of the Kochen-Specker theorem was done with neutrons by Bartosik, Klepp, Schmitzer, Sponar, Cabello, Rauch, and Hasegawa[4].

[1] I.e. a theory based on local-realism.

Objective reality:
The concept of objective reality springs from the idea that there exists elements of reality. “If without in any way disturbing a system, we can predict with certainty (i.e., with probability equal to unity) the value of a physical quantity, then there exists an element of physical reality corresponding to this physical quantity.”

Locality:	Non-contextuality:
The concept of locality springs from the theory of relativity, or more precicely from the postulate that nothing can travel faster than the speed of light. Thus a particle at position A can only have information about a particle at position B if the information has had time to be transmitted the distance from B to A at the speed of light. “But on one supposition we should, in my opinion, absolutely hold fast: the real factual situation of the system S_2 is independent of what is done with the system S_1, which is spatially separated from the former.” [1]	The concept of non-contextuality comes from the notion that given three observables A, B, and C, where the outcome of A is not affected by neither the outcome of B nor C (the outcome of these latter two can affect each other though), then the outcome of A is not affected by if it is measured with B or C.[2]

Figure 1.4: These information boxes has been presented before in my Licentiate thesis.

[1] A. Einstein in Albert Einstein, Philosopher Scientist, (Edited by P. A. Schilp) p.85, Library of Living Philosophers, Evanston, Illinois (1949).

[2] The act of measuring A with B is one context, and measuring A with C another.

1.6 Graphs

Graphs are a convenient tool to use when working with noncontextuality inequalities, they will also be some sort of theme for this thesis. We will talk about two different but related kind of graphs; the orthogonality graphs and the exclusivity graphs. An orthogonality graph is a set of vertices and edges, where an edge connects two vertices if they are orthogonal. An exclusivity graph is a set of vertices and edges, where an edges connects two vertices if they are exclusive. What do we mean when we say that two vertices are orthogonal or exclusive? To start with we associate the vertices to, in the case of orthogonality graphs, unit-vectors or, in the case of exclusivity graphs, probabilities for events. Now, an orthogonality graph shows the orthogonality relation between the set of unit-vectors and an exclusivity graph shows the exclusivity relations of the set of events, we say that two events are exclusive if they cannot both be true simultaneously.

From graph theory we can learn some properties of graphs which are useful in our study of noncontextuality inequalities. A fundamental property of a graph G is the independence number, $\alpha(G)$. $\alpha(G)$ is the largest set of independent vertices in G, two vertices are independent if they are not connected by an edge. Calculating $\alpha(G)$ is a NP-hard problem so another property of the graph G, the Lovász number $\vartheta(G)$, which is an upper bound of $\alpha(G)$ was found, and this is computable in polynomial time. $\vartheta(G)$ is defined as $\vartheta(G) = \max \sum_{i=1}^{n} |\langle\psi|v_i\rangle|^2$,[1] and this is of course the sum of the expectation values of the projectors $|v_i\rangle\langle v_i|$.

[1]The maximization is done over the different sets of $|v_i\rangle$s that fulfill the graph, these are called orthogonal representations of the graph, and all $|\psi\rangle$s.

1.7 Units of quantum information

Information is always carried by and stored in some kind of physical system, the system of choice depends on the application and can vary from scratches on bark to the direction of the current in a fluxqubit. In this thesis we will use spatial and polarisation degrees of freedom of photons, these photons should come one at a time and as such be treated like single quantum particles. This is not really true since a proper single photon source was not available when the experiments were done. Instead we used an approximation to a single photon in the guise of attenuated coherent light. The reason we need a single quantum particle is the assumptions we will make that a particle can contain more information than a classical description allows[1]. Mathematically we can write it $|\psi\rangle$, for a single particle state, $|\psi_1, \psi_2\rangle$, for a two particle state, and so on. Now the smallest system that can contain information is a two dimensional one[2], this is in classical information theory called a binary digit, bit for short, and the quantum informational counterpart is called a quantum bit (qubit). States containing quantum information lives in Hilbert space[3], the dimension of the Hilbert space needed for distinguishing the different states in use is the dimension of the information carrying entity.

A general qubit can be written as $a|0\rangle + be^{i\varphi}|1\rangle, a, b \in \mathbf{R}$, the reason that a and b are real is that the global phase of a state is a free parameter and has no physical meaning. The states are usually normalized, this means that the square of the coefficients a and b add to one $a^2 + b^2 = 1$ and is done to simplify calculations[4]. Thanks to the fact that Hilbert space is complex, a qubit is not defined only by the relative amplitudes of $|0\rangle$ and $|1\rangle$, but also the relative phase φ. This means that (pure) states live on a two dimensional surface in a three dimensional space, called the Bloch sphere[5].

[1] It would not have mattered if we used 1, 2, or 100 particles as long as we could know for sure that was the exact number we were using, but since knowing the exact number of particles is a difficult task using one particle is the easiest.

[2] This represents that something is or is not, a one dimensional system only has one state and can not contain information since information only lives in relation to something else.

[3] Hilbert space is a complex space with a metric and an innerproduct.

[4] The magnitude of a state only holds meaning if it can be compared to something else, of which there is none for a single state.

[5] Mixed states live in the Bloch ball, but that is another story altogether.

Part II

Experiments

2. Bell

We will start this journey of experimental quantum optics and quantum information with a theoretical chapter. The resource that most clearly represent the quantumness in quantum information is entanglement. The discussion of entanglement started with a paper by Einstein, Podolsky, and Rosen[1] where they claimed that quantum mechanics is either incomplete or incorrect. This led to the EPR-paradox and the subsequent discussion between Einstein and Bohr. Bell was inspired by the idea that it might be possible to design an experiment[5] for which quantum mechanics would predict a value unreachable by the classical point of view (represented by Einstein et al). He used the notion of LHVTs, which have the property of local-realism (see boxes about locality and objective-reality in Sec. (1.5)), to construct a function of the expectation values of some specific observables. This fuction was bounded from above, however the bound was surpassed by quantum mechanics. Clauser, Horne, Shimony, and Holt [6] generalized the result of Bell and constructed an inequality (the CHSH-inequality) which was experimentally testable. So physicists were now provided with a way to show or solve the EPR-paradox. This was done by Freedman and Clauser[2] as well as by Aspect, Grangier, Roger, and Dalibard[7–9] using entangled photons from a calcium cascade source.

2.1 Derivation of the CHSH-inequality

In the original article by Bell he showed that it is possible to construct situations where a LHVT cannot correctly reproduce the predictions of quantum mechanics. His argumentation is based on a Gedankenexperiment presented by Bohm and Aharonov[10], which basically is the EPR-experiment in a simplified form. While fundamentally important, the aim of Bell's article was not to suggest an experiment which could prove if the world is describable by LHVTs or quantum mechanics, just that such an experiment can be constructed. Clauser, Horne, Shimony, and Holt[6] presented a generalization of Bell's theorem and subsequently a proposition for an experiment which could make the distinction between LHVTs and quantum mechanics. They chose the experimental setting to consist of two parties, Alice and Bob, who can choose between two different measurement settings, $x \in \{a, a'\}$ and $y \in \{b, b'\}$. Further, pairs of particles are sent to the two parties, one particle to each. Upon measurement the results *A(x)* and *B(y)*, with possible values ± 1, are recorded. Assume that there is a LHVT that can describe this system, then the measurement outcomes could be written $A(x,\lambda)$ and $B(y,\lambda)$, where λ is the hidden variable. Note that since we assume that the theory is local $A(x,\lambda)$ must be independent of y and $B(y,\lambda)$ independent of x. We can now define the correlation between A and B as:

$$C_{AB}(x,y) = \int_\Lambda A(x,\lambda)B(y,\lambda)\rho(\lambda)d\lambda,$$

where $\rho(\lambda)$ is the probability distribution of λ, for $\lambda \in \Lambda$[1]. Now consider:

$$\begin{aligned}
\left|C_{AB}(a,b') - C_{AB}(a,b)\right| &\leq \int_\Lambda \left|A(a,\lambda)B(b',\lambda) - A(a,\lambda)B(b,\lambda)\right| \rho(\lambda)d\lambda \\
&= \int_\Lambda \left|A(a,\lambda)B(b',\lambda)\right| (1 - B(b',\lambda)B(b,\lambda))\rho(\lambda)d\lambda \\
&= \int_\Lambda (1 - B(b',\lambda)B(b,\lambda))\rho(\lambda)d\lambda \\
&= 1 - \int_\Lambda B(b',\lambda)B(b,\lambda)\rho(\lambda)d\lambda.
\end{aligned}$$

Let us make another setting *a'* which has the correlation $C_{AB}(a',b') = 1-\delta$, where $0 \leq \delta \leq 1$. We can now divide the set Λ into $\Lambda_\pm = \{\lambda \,|A(a',\lambda) = \pm B(b',\lambda)\}$[2],

[1] Λ contains all knowledge that can be preestablished for the system.

[2] I.e., we separate the HVs for which A and B are correlated from those for which they are anticorrelated.

it follows that $\int_{\Lambda_-}\rho(\lambda)d\lambda = \frac{1}{2}\delta$. Now we can write:

$$\begin{aligned}
\int_\Lambda B(b',\lambda)B(b,\lambda)\rho(\lambda)d\lambda &= \int_{\Lambda_+} A(a',\lambda)B(b,\lambda)\rho(\lambda)d\lambda - \int_{\Lambda_-} A(a',\lambda)B(b,\lambda)\rho(\lambda)d\lambda \\
&= \int_{\Lambda_+} A(a',\lambda)B(b,\lambda)\rho(\lambda)d\lambda + \int_{\Lambda_-} A(a',\lambda)B(b,\lambda)\rho(\lambda)d\lambda \\
&\quad -2\int_{\Lambda_-} A(a',\lambda)B(b,\lambda)\rho(\lambda)d\lambda \\
&= \int_\Lambda A(a',\lambda)B(b,\lambda)\rho(\lambda)d\lambda - 2\int_{\Lambda_-} A(a',\lambda)B(b,\lambda)\rho(\lambda)d\lambda \\
&\geq \int_\Lambda A(a',\lambda)B(b,\lambda)\rho(\lambda)d\lambda - 2\int_{\Lambda_-} \left|A(a',\lambda)B(b,\lambda)\right|\rho(\lambda)d\lambda \\
&= \int_\Lambda A(a',\lambda)B(b,\lambda)\rho(\lambda)d\lambda - 2\int_{\Lambda_-} \rho(\lambda)d\lambda \\
&= C_{AB}(a',b) - \delta
\end{aligned}$$

thus we have:

$$\begin{aligned}
\left|C_{AB}(a,b') - C_{AB}(a,b)\right| &\leq 1 - \int_\Lambda B(b',\lambda)B(b,\lambda)\rho(\lambda)d\lambda \\
&\leq 1 - C_{AB}(a',b) + \delta \\
&= 2 - C_{AB}(a',b) - (1-\delta) \\
&= 2 - C_{AB}(a',b) - C_{AB}(a',b')
\end{aligned}$$

and we finally end up with the inequality:

$$\left|C_{AB}(a,b') - C_{AB}(a,b)\right| + C_{AB}(a',b) + C_{AB}(a',b') \leq 2$$

or as it usually is written:

$$\left|C_{AB}(a',b') + C_{AB}(a,b') - C_{AB}(a,b) + C_{AB}(a',b)\right| \leq 2.$$

Now let us look at another way of deriving the inequality, starting with the exclusivity graph, see Fig. (2.1), introduced by Cabello, Severini, and Winter[11]. From this we can construct the inequality:

$$\begin{aligned}
S_{CHSH} =& P(11|00) + P(00|00) + P(11|10) + P(00|10) \\
&+ P(10|11) + P(01|11) + P(11|01) + P(00|01) \leq 3
\end{aligned}$$

where $P(ab|xy)$ is the probability that the observables A_x and B_y take the values $(-1)^a$ and $(-1)^b$, $x \in \{0,1\}$ and $y \in \{0,1\}$ are the settings. From the probabilities $P(ab|xy)$ we can construct expectation values of the observables:

$$\langle A_x B_y \rangle = P(11|xy) + P(00|xy) - P(10|xy) - P(01|xy).$$

Now if we instead look at the expectation values:

$$\left\langle \mathbb{1} + (-1)^{a+b} A_x B_y \right\rangle = 2(P(ab|xy) + P(\bar{a}\bar{b}|xy)),$$

and group the probabilities of the inequality by which measurements they belong to we can make the identification:

$$\begin{aligned}
&[P(11|00) + P(00|00)] + [P(11|10) + P(00|10)] \\
+&[P(10|11) + P(01|11)] + [P(11|01) + P(00|01)] \\
=&\frac{1}{2}\left(\langle \mathbb{1} + A_0 B_0 \rangle + \langle \mathbb{1} + A_1 B_0 \rangle + \langle \mathbb{1} - A_1 B_1 \rangle + \langle \mathbb{1} + A_0 B_1 \rangle\right) \\
=&\frac{1}{2}\left(4 + \langle A_0 B_0 \rangle + \langle A_1 B_0 \rangle - \langle A_1 B_1 \rangle + \langle A_0 B_1 \rangle\right) \\
\leq& 3,
\end{aligned}$$

which finally gives us:

$$\langle A_0 B_0 \rangle + \langle A_1 B_0 \rangle - \langle A_1 B_1 \rangle + \langle A_0 B_1 \rangle \leq 2.$$

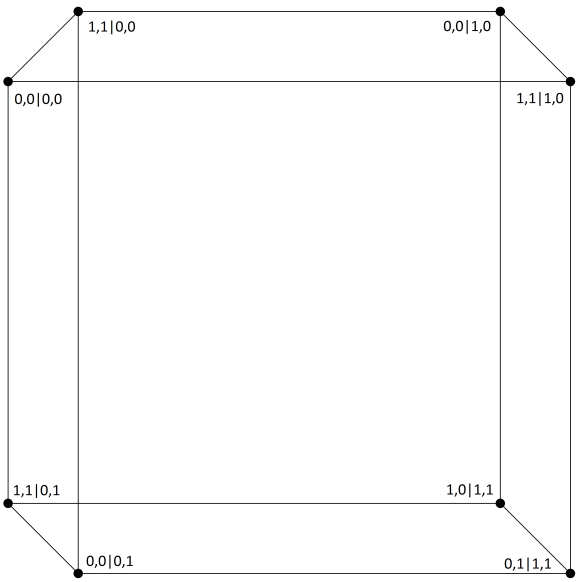

Figure 2.1: The exclusivity graph for S_{CHSH}.

3. Bell Dimension Witness

The first experiment we will discuss is the implementation of a dimension witness inspired by the CHSH-inequality[6].

A dimension witness is a mathematical function of operators that yields different values depending on the dimension of the states on which the operators acts. The higher the dimension the larger is the value that can be obtained. Please note that these values are the maximal values obtainable, thus a dimension witness can only give a lower bound of the dimension (a higher dimensional state can pose as a lower dimensional one). This means that a dimension witness cannot be used to detect possible side channels[1] for example. This chapter is based on one of the experiments described in Paper I.

[1] Side channel attacks is a collective name for attacks on communication schemes where the adversary introduces additional degrees of freedom (side channels) in order to extract information from the communicating parties.

3.1 Motivation

The idea of constructing witnesses for the dimension of quantum systems was conceived by Brunner et. al. in 2008[12]. They took a black-box approach and considered correlations beween separated measurement devices. In 2010, Gallego et. al.[13] took this idea and made it device-independent[1] by looking at the outcomes conditioned on the setting of the state preparation and the measurement. Here we will discuss a dimension witness inspired by the device-independent idea but which actually emerges when one translates a device-independent protocol, based on the CHSH-inequality, to a semi-device-independent[2] one[14]. This has the advantage that the states and measurements are chosen for their applicability in quantum key distribution and/or quantum random-number-generation protocols.

[1]Device-indenpendence means that the communicating parties either do not know the inner workings of their devices or do not trust them.

[2]Semi-device-independence means that the communicating parties have some level of trust in their devices, even if they do not have complete control over the inner workings.

3.2 Derivation

The starting point of the derivation of the dimension witness in this chapter is a two partite device independent protocol[14]. The two parties, say Alice and Bob, each get one particle of a maximally entangled pair. They randomly choose to make one out of two predefined measurements each and record the outcome. The security of this protocol comes from the fact that by randomly choosing joint events[1], they can construct a CHSH-inequality and if they violate the classical bound nobody has intercepted their particles since the entanglement is still there, i.e., their communication is secure.

Let the measurement settings of Alice and Bob be x' and y, respectively, and their outcomes be a and b. Their joint probability for the different outcomes can now be expressed as: $P(a,b|x',y)$ and the CHSH-inequality as:

$$S = \sum_{a,b,x',y} \alpha_{a,b,x',y} P(a,b|x',y).$$

Now consider a similar situation where instead of the two parties having a distributed entangled state, one of them sends single particles to the other one. Let Alice be the sender and thus not have a measurement outcome, this can be modeled as Alice choosing a measurement and getting an outcome which in turn is the setting for the sender device. The outcome probability for Bob can now be expressed as: $P(b|a,x',y)P(a|x')$ where the initial choice and resulting outcome for Alice gives the new setting $(a,x') = x$. Since x' is chosen randomly and unweighted: $P(a|x') = \frac{1}{A}$ where A is the size of the alphabet of a and the witness function corresponding to the CHSH-inequality will then take the form:

$$D = \sum_{a,b,x',y} \frac{\alpha_{a,b,x',y}}{A} P(b|a,x',y)$$

where $(a,x') = x$ and can thus be written:

$$D = \sum_{b,x,y} \beta_{b,x,y} P(b|x,y).$$

This is the general formula and we will now discuss the specific expression of the dimension witness presented in this chapter.

[1] Occations where both Alice and Bob detects a particle.

The measurements in the CHSH-inequality are dichotomic, i.e., they can take the values -1 or 1, and since Alice and Bob choose one out of two measurements each they end up with 16 different outcome probabilities which in order to get the greatest violation should have coefficients as shown below:

$P(1,1\|x_1',y_1)$	$-P(1,1\|x_1',y_2)$	$P(1,1\|x_2',y_1)$	$P(1,1\|x_2',y_2)$
$-P(1,-1\|x_1',y_1)$	$P(1,-1\|x_1',y_2)$	$-P(1,-1\|x_2',y_1)$	$-P(1,-1\|x_2',y_2)$
$-P(-1,1\|x_1',y_1)$	$P(-1,1\|x_1',y_2)$	$-P(-1,1\|x_2',y_1)$	$-P(-1,1\|x_2',y_2)$
$P(-1,-1\|x_1',y_1)$	$-P(-1,-1\|x_1',y_2)$	$P(-1,-1\|x_2',y_1)$	$P(-1,-1\|x_2',y_2)$

This will translate to the outcome probabilities of the witness function, with $(1,x_2') = x_1$, $(-1,x_2') = x_2$, $(1,x_1') = x_3$, and $(-1,x_1') = x_4$ (the colors indicate corresponding terms):

$P(1\|x_1,y_1)$	$-P(-1\|x_1,y_1)$	$P(1\|x_1,y_2)$	$-P(-1\|x_1,y_2)$
$-P(1\|x_2,y_1)$	$P(-1\|x_2,y_1)$	$-P(1\|x_2,y_2)$	$P(-1\|x_2,y_2)$
$P(1\|x_3,y_1)$	$-P(-1\|x_3,y_1)$	$-P(1\|x_3,y_2)$	$P(-1\|x_3,y_2)$
$-P(1\|x_4,y_1)$	$P(-1\|x_4,y_1)$	$P(1\|x_4,y_2)$	$-P(-1\|x_4,y_2)$

Now the expectation values $E_{xy} = P(1|x,y) - P(-1|x,y)$ can be constructed and give the expression:

$$D = (E_{x_1y_1} + E_{x_1y_2}) - (E_{x_2y_1} + E_{x_2y_2}) \tag{3.1}$$
$$+ (E_{x_3y_1} - E_{x_3y_2}) - (E_{x_4y_1} - E_{x_4y_2}) \tag{3.2}$$

for the witness function.

Since the basis for this witness is a communication protocol we choose the four states, that Alice can emit, to be the BB84[15] states with the following correspondence: $x_1 \Rightarrow |1\rangle$, $x_2 \Rightarrow |0\rangle$, $x_3 \Rightarrow \frac{1}{\sqrt{2}}(|0\rangle + |1\rangle)$, and $x_1 \Rightarrow \frac{1}{\sqrt{2}}(|0\rangle - |1\rangle)$ and in order to get as large violation as possible we need to optimize the measurements y for Bob.

A general dichotomic measurement can be written as:

$$M_i = \mathbb{1} - 2\sum |m_i\rangle\langle m_i| \tag{3.3}$$

where $\sum |m_i\rangle\langle m_i|$ represents[1] the eigenstates with eigenvalue -1.

[1]N.B. the index i referes to the measurement not to the eigenstate of the measurement, i.e., it is not a summation index.

3.3 Setup

We have seen that the witness can distinguish between bits, qubits, trits, qutrits, and quarts. Thus in order to test this witness we will need to be able to prepare states belonging to these classes. A nit is just an n level system without phase relation, while a qunit is an n level system with phase relation. This means that we need a physical system of at least four levels where we should be able to set a phase between at least three of these. We have chosen to encode our *nits in two spatial- and two polarization degrees of freedom. An overview of the setup is given in Fig. (3.1).

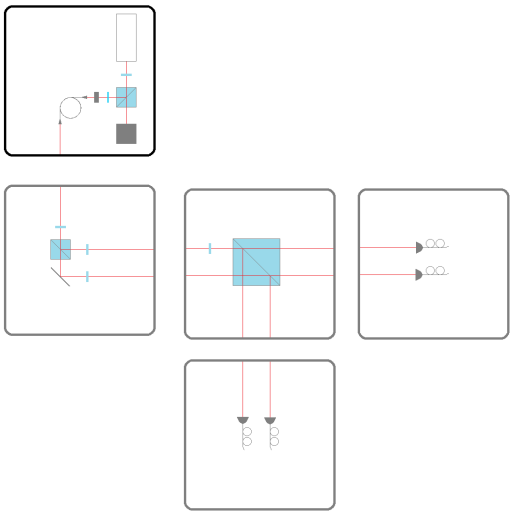

Figure 3.1: The setup for the CHSH-inspired dimension witness.

The P-box

In order to prepare a single photon state we need a source of single photons. The single photon source used in this experiment consists of a highly attenuated laser. A laser emits photons in a coherent state, this means that they are in a coherent superposition of all Fock-states[1]. By attenuation we can shift the expectation value of the number operator to be significantly lower than one, this will then yield a state where multiphoton events are very rare while single photon events still occur relatively often. The attenuation is done in two steps, first a HWP and a PBS make up a variable attenuator, then an optical density (OD) filter does the main attenuation. In the single photon source there is also an additional QWP just before the OD-filter, this is in place to rotate the polarization of any reflections from the OD-filter and fiber coupler so that they cannot pass the same way through the PBS back to the laser[2]. When the photon state has been attenuated it is coupled to a single mode optical fiber. The fiber has a passive polarization controller attached so that the photon source can be made to produce single photons vertically polarized in a single spatial mode, see Fig. (3.2). Now we want to expand the state to two spatial modes, this is done by a HWP and a PBS whereby the state

$$|\psi\rangle = \sin(2\theta_1)\,|a\rangle + \cos(2\theta_1)\,|b\rangle \tag{3.4}$$

can be produced[3]. In each of the two spatial modes there are additional HWPs to expand the state to

$$\begin{aligned} |\psi\rangle = \quad & \sin(2\theta_1)\cos(2\theta_2)\,|H,a\rangle + \sin(2\theta_1)\sin(2\theta_2)|V,a\rangle \\ & + \cos(2\theta_1)\cos(2\theta_3)|H,b\rangle + \cos(2\theta_1)\sin(2\theta_3)|V,b\rangle. \end{aligned} \tag{3.5}$$

This state has access to four levels by adjusting the angle θ_i of the HWPs, see Fig. (3.3), and thus has the possibility to constitute a quart. Since we only use HWPs, and not QWPs, all coefficients in the state will be real numbers. This is not a problem for the experiments since all the states needed both for aligning the measurements and for testing the inequalities have coefficients which are real. Now that a state of four levels can be created we can define the laboratory basis:

$$\begin{aligned} |0\rangle \equiv |H,b\rangle, \quad |1\rangle \equiv |V,a\rangle \\ |2\rangle \equiv |H,a\rangle, \quad |3\rangle \equiv |V,b\rangle. \end{aligned} \tag{3.6}$$

[1] $|\psi\rangle = \sum_{k=0}^{\infty} a_k e^{i\varphi_k}\,|k\rangle$, where the a_k's are the probability amplitudes for the different Fock-states, and the φ_k's are the relative phases.

[2] Reflections that go straight back into the laser cavity can make the laser unstable.

[3] Note that the polarization in mode a is horizontal while in b it is vertical.

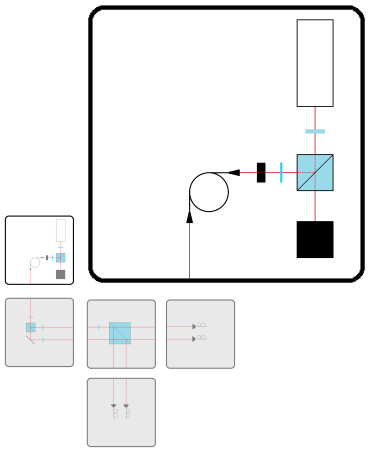

Figure 3.2: The source of emulated single photons. Directly after the laser we have a HWP to regulate the fraction reflected in the PBS (this works as a variable attenuator). Before the OD-filter we have a QWP so that any reflections from the filter or the fiber coupler will be turned to horizontal polarization and thus transmitted by the PBS. The optical fiber goes through a passive polarization controller so that we can set the polarization as we want it. This setup gives us nearly single photons in a single spatial mode and a set polarization mode.

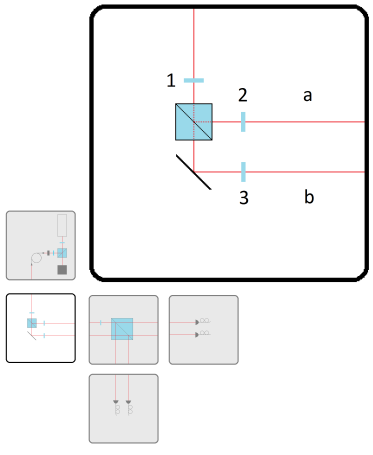

Figure 3.3: Preparation of quantum states. A HWP turns the polarizations so that we can distribute the photon state over our two spatial modes. The two spatial modes both have HWPs in order to distribute the photon state over the polarization modes.

The U-box

The measurements in this experiment are all dichotomic, and the two outcomes for each measurement is determined by the sign of the eigenvalue of the eigenstates of the corresponding observable. With the encoding we have chosen and the measurements we need to perform, all transformations can be done with a HWP in mode a, see Fig. (3.4), resulting in the following:

$$\begin{aligned} |-\rangle &\equiv |V,a\rangle \\ |+\rangle &\equiv \alpha\,|H,a\rangle + \beta\,|H,b\rangle + \gamma|V,b\rangle \end{aligned} \tag{3.7}$$

The E-box

When the state has been rotated by the U-box the negative-valued eigenstate of the observable will be $|m_i\rangle = |V,a\rangle$ in all measurements except for the quart, where $|m_i\rangle = |H,b\rangle$ and $|m_i\rangle = |V,b\rangle$. Thus a PBS in mode a, see Fig. (3.4), will entangle the negativ-valued eigenstate with spatial mode a and the positive-valued ones with the spatial modes b, c, and d.

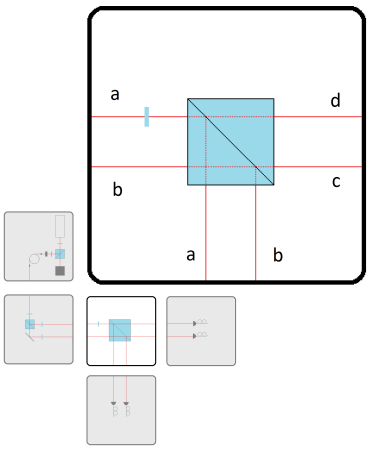

Figure 3.4: Unitary transformation from laboratory basis to the eigenbasis of the operator and entangling the eigenstates with spatial modes. The HWP in mode a makes the transformation from the laboratory basis and the PBS entangles the eigenstates with different spatial modes.

The D-box

In this experiment the D-box consists of three single photon detectors, one in each output mode of the E-box.

3.4 Results

The aim for the experimental implementation of the CHSH inspired dimension witness was to reproduce the theoretical values for systems of different dimensions. The maximum values for classical states have been derived for the general dimension witness of this kind and were given as: $D(bit) = 4$ for bits, $D(trit) = 6$ for trits, and $D(nit) = 8$ for all higher dimensional systems[1]. The maximum values for sets of quantum states were found in the optimization process for the specific witness: $D(qubit) = 5.66$ for qubits and $D(qutrit) = 6.47$ for qutrits. Our experimental results are presented in the table (3.1), D_{th} are the theoretical value, D_{exp} are the raw experimental values, and D^b_{exp} are the experimental values corrected for dark counts in the detectors. We also include the errors of the experiment as: Δ_p for the error induced by polarizing components[2], Δ_d for errors due to poissonian counting statistics, and Δ_T for the total errors.

Table 3.1: Experimental results for test of the CHSH inspired dimension witness, D_{th} are the theoretical bounds, D_{exp} are the experimental values for these bounds, and D^b_{exp} are the experimental values corrected for dark counts in the detectors. Δ_p are the errors due to polarizing components, Δ_d are the errors due to poissonian statistics, and Δ_T are the total errors. **The colored columns contain the numbers of greatest interest, the theoretical bounds, the corrected experimental values, and the total errors**.

Input states	D_{th}	D_{exp}	D^b_{exp}	Δ_p	Δ_d	Δ_T
bit	4.00	3.94	3.98	0.08	0.010	0.08
qubit	5.66	5.51	5.56	0.12	0.008	0.12
trit	6.00	5.90	5.96	0.13	0.010	0.13
qutrit	6.47	6.44	6.50	0.14	0.009	0.14
nit	8.00	7.88	7.94	0.16	0.010	0.16

[1] This is the algebraic limit.

[2] I.e., non-perfect alignment of wave-plates and imperfect splitting by PBSs.

4. Optimal Dimension Witness

In this chapter we will discuss a family of optimal dimension witnesses[13]. These are, in contrast to the CHSH-based witness, constructed to give as large separation between all the bounds, for the different dimensions, as possible.

This family of dimension witnesses was found by Gallego, Brunner, Hadley, and Acín[13]. This chapter is based on one of the experiments described in Paper II.

4.1 Motivation

As was described in the last chapter dimension witnesses have evolved over time and the type discussed in this chapter is of the device-independent type. However instead of being tailored for communication protocols these are optimized for discrimination between dimension bounds. The family of dimension witnesses described in this chapter also have the advantage that there is a formula for deriving witnesses which can distinguish between any dimensions[1].

[1]The higher the dimensions you want to distinguish between, the larger the witness function will be.

4.2 Derivation

In contrast to the dimension witness in the last chapter where we have started the derivation from a comunication protocol, the derivation of these witnesses starts from the set of possible classical experiments that have a deterministic outcome. An experiment with N states and m measurements is here defined by a vector $E = (E_{11}, E_{12}, \ldots, E_{1m}, E_{21}, \ldots, E_{Nm})$, where $E_{xy} = P(1|x,y) - P(-1|x,y)$ is the expectation value of measurement y given the state x. Any possible experiment can be written as a convex combination of the set of deterministic experiments, and a deterministic experiment has all $E_{xy} = \pm 1$. The set of all possible experiments constitute a polytope, $\mathbb{P}_{Nm}$, with the deterministic experiments as extremal points. A set of states with dimension larger than N can be used to realize all experiments in $\mathbb{P}_{Nm}$, while a set of states with dimension d less than N can realize experiments constituting the polytope $\mathbb{P}^d_{Nm}$ which is completely enclosed in $\mathbb{P}_{Nm}$. The facets of this new polytope can be written as linear combinations of the expectation values E_{xy} and are bounded by a number, C_d, dependent on the dimension d. This is what is called a tight classical dimension witness[1]. When trying to do the same thing as above for a set of quantum states you end up in a bit of trouble because while the set of possible experiments is convex it does not constitute a polytope since there is an infinite number of extremal points and there is no analogue to the facets that define the classical dimension witness. However, when looking at the simplest classical case, $\mathbb{P}^2_{32}$, it can be shown that it exhibits only one type of nontrivial facet which gives the classical dimension witness

$$I_3 = |E_{11} + E_{12} + E_{21} - E_{22} - E_{31}| \leq 3. \tag{4.1}$$

The first four terms can be seen as the CHSH terms giving, for a two level quantum system, a maximum of $2\sqrt{2}$ and the last term is given by a third state which can be chosen freely and thus can be made to yield -1. Optimizing for general quantum states and operators you can find that the maximum value for a set of qubits is $1+2\sqrt{2}$ and thus a dimension witness capable of distinguishing between bits, qubits, and higher dimensional sets of states has been found. The dimension witness has been generalized to distinguish higher dimensional states by making the expansion of I_3 for $N = m+1$ as:

$$I_N \equiv \sum_{j=1}^{N-1} E_{1j} + \sum_{i=2}^{N} \sum_{j=1}^{N+1-i} \alpha_{ij} E_{ij}, \qquad \alpha_{ij} = \begin{cases} 1, & i+j \leq N \\ \text{-1}, & i+j > N \end{cases} \tag{4.2}$$

it can be shown that for sets of classical states, $I_N \leq C_d = \frac{N(N-3)}{2} + 2d - 1$.

[1] It is a classical dimension witness because in order to violate C_d a set of states with dimension at least $d+1$ is needed, and it is tight because it lays tight against a facet of the polytope.

4.3 Setup

The setup for this experiment is the same as in the previous one except for the U-box, see Fig. (4.1).

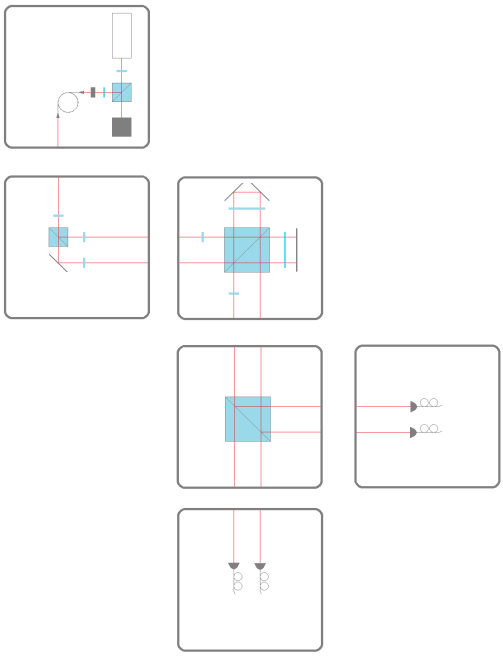

Figure 4.1: The setup of the optimal dimension witness.

The U-box

As in the previous experiment all measurements are dichotomic, and the two outcomes for each measurement is determined by the sign of the eigenvalue of the eigenstates of the corresponding observable. However, due to the states being slightly different we need a more complicated unitary transformation, see Fig. (4.2). In addition to the HWP in mode a, a twisted polarizing Michelson interferometer is used to move the vertical components of each spatial mode to the other, and changing all polarizations from horizontal to vertical and vice versa. In the new b mode another HWP is placed in order to interfere the polarizations modes resulting in the following:

$$\begin{aligned} |-\rangle &\equiv |H,b\rangle \\ |+\rangle &\equiv \alpha\,|V,a\rangle + \beta\,|V,b\rangle. \end{aligned} \tag{4.3}$$

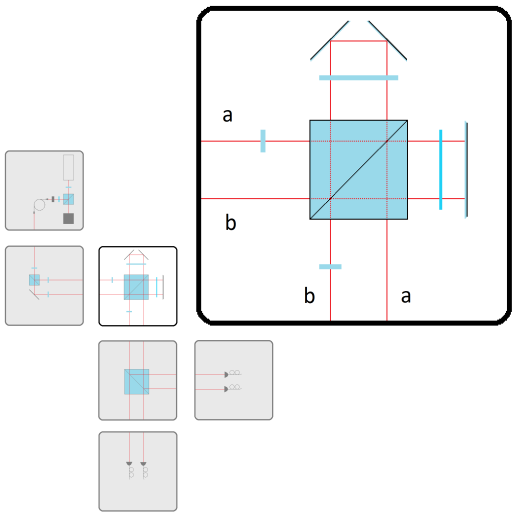

Figure 4.2: Unitary transformation from the laboratory basis to the eigenbasis of the operator. The first HWP interferes the polarization modes in mode a. The polarizing Michelson interferometer transfere the $|V,a\rangle$-component to $|H,b\rangle$, $|H,a\rangle$ to $|V,a\rangle$, and $|H,b\rangle$ to $|V,b\rangle$. Finally, the second HWP interferes the polarization modes in mode b.

The E-box

As seen above the U-box rotates the state so that the negative-valued eigenstate of the observable will be $|m_i\rangle = |H,b\rangle$. A PBS in mode b will then entangle the negative-valued eigenstate with spatial mode b and the positive-valued ones with the spatial modes a and c, see Fig. (4.3).

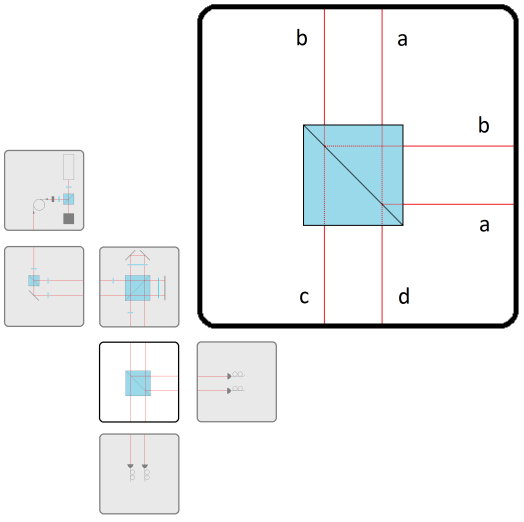

Figure 4.3: Entangling the eigenstates with different spatial modes. The PBS splits the polarization modes of mode b into different spatial modes.

The D-box

The d-box consists of single photon detectors in the modes a, b, c, and d.

4.4 Results

The optimal dimension witness was designed to get a scalable dimension witness capable of distinguishing between classical and quantum sets of states. The goal of the experiment was to reproduce the classical and quantum bounds as well as possible. The formula for the classical bounds as stated in chapter 4.2 is: $I_N \leq C_d = \frac{N(N-3)}{2} + 2d - 1$, and yields for the witness with three different state preparations: $I_3(bit) = 3$ for bits and $I_3(nit) = 5$ for higher dimensional sets of states. For the witness with four different state preparations we get: $I_4(bit) = 5$ for bits, $I_4(trit) = 7$ for trits, and $I_4(nit) = 9$ for higher dimensional sets of states. The bounds for quantum mechanical sets of states were found during the optimization process for the states and operators: $I_3(qubit) = 1 + 2\sqrt{2} \approx 3.8284$ and $I_4(qubit) = 6$ for qubits, and $I_4(qutrit) = 2 + \sqrt{13 + 16\sqrt{2}} \approx 7.9688$ for qutrits. Our experimental results are presented in table (4.1)[1].

Table 4.1: Experimental results for test of the optimal dimension witnesses. I_{th} is the theoretical value, I_{exp} the raw experimentally measured value, I^b_{exp} is the experimentally measured value with subtracted dark counts, Δ_T is the total experimental error, Δ_p the error due to misaligned polarizing components, and Δ_d the error due to the poissonian counting statistics from the detectors. **As before the colored columns are of most interest, the theoretical value, the experimentally measured value with subtracted dark counts, and the total experimental error**.

	Input states	I_{th}	I_{exp}	I^b_{exp}	Δ_p	Δ_d	Δ_T
I_3	qubit	3.83	3.65	3.78	0.0772	0.0125	0.08
	nit	5.00	4.71	4.93	0.1021	0.0150	0.10
I_4	BB84	5.65	5.52	5.55	0.1126	0.0133	0.11
	qubit	6.00	5.76	5.95	0.1221	0.0163	0.12
	trit	7.00	6.76	6.96	0.1433	0.0171	0.14
	qutrit	7.97	7.29	7.60	0.1596	0.0419	0.17
	nit	9.00	8.52	8.91	0.1833	0.0209	0.18

[1]This table has previously been presented in my Licentiate thesis.

5. Kochen-Specker

This chapter will not present an experiment. It is a theoretical chapter with the purpose of introducing contextuality, which will be the theme for the rest of the thesis. So far we have taken a look at Bell inequalities which were designed to show that LHVT cannot explain the outcomes of some experiments. Then we looked at dimension witnesses based on the CHSH-inequality, how they are constructed by taking the two particle experiment with two recievers to a one particle experiment with one sender and one receiver, where the state preparation setting can be seen as a result of a measurement setting and measurement outcome. This shows that while we can test the validity of LHVT by the use of Bell-inequalities, if we remove the possibility of two partite entanglement, we can still measure some kind of quantumness by making consecutive measurements of certain observables.

5.1 The Kochen-Specker rules

In order to show that quantum mechanical predictions cannot be described by NCHVTs Kochen and Specker derived two rules[3] for systems with three or more degrees of freedom which have to be fulfilled by any NCHVT.

- Two orthogonal vectors cannot both be '1'.
- Exactly one vector in all completely connected n-lets is '1', where n is the degrees of freedom of the system considered.

Even without the mathematical proof we can see that this is reasonable if we project a state onto the projectors defined by the vectors represented by the vertices of a graph.

Consider a completely connected orthogonality graph with three vertices, this is a representation of a set of basis vectors in a three-dimensional states-pace. According to HVTs there should exist an element of objective reality to all possible measurements. Assume that our three basis vectors represent three possible outcomes of a specific measurement, and that a projection onto one of the vectors signifies a measurement result. Clearly we will always project on some vector, and likewise we can only project on one of the vectors.

If we now could construct a graph in which these rules cannot be fulfilled we have proven that quantum mechanical predictions cannot be described by NCHVTs.

5.2 The original Kochen-Specker graph

The original Kochen-Specker graph is composed of 120 vertices, when representing the vertices by vectors it is found that three vectors are repeated once each, resulting in 117 vectors, see Fig. (5.1). This graph was the first graph that was shown not to fulfill the Kochen-Specker rules, no matter how we try to assign values to the vertices we will always have a conflict with the rules when trying to assign a value to (at least) the last vertex.

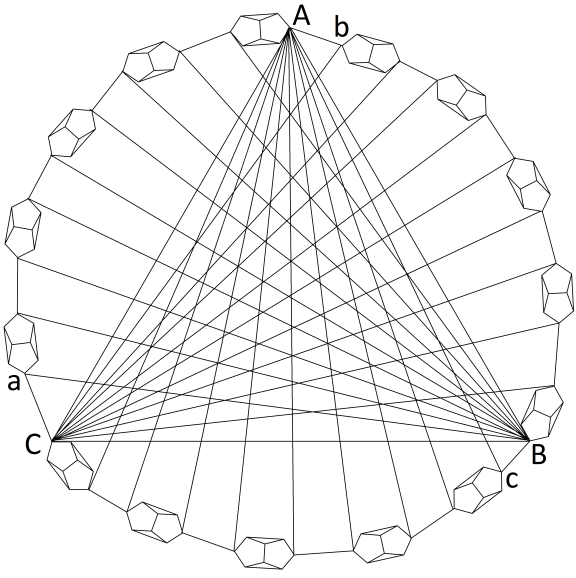

Figure 5.1: The Kochen-Specker graph, vertices A and a, B and b, and C and c, represents the same vector respectively.

6. KCBS

This chapter will take us into the world of experimental violation of non-contextual inequalities.

The inequality we will discuss is the KCBS-inequality[1], the simplest non-contextual inequality violated by quantum mechanics. This chapter is based on one of the experiments described in Paper III.

[1]Named after Klyachko, Can, Biniocioğlu, and Shumovsky.

6.1 Motivation

As we saw in the last chapter non-classical correlations can be obtained even in the absence of entanglement. The Kochen-Specker theorem gives us a way to construct state-independent tests of NCHVTs. If we instead are interested in the minimal test of NCHVTs we have to abandon state-independence and consider an inequality violated by certain states. Klyachko, Can, Binicioğlu, and Shumovsky[16] found that it is possible to use the pentagon graph[1], see Fig. (6.1), to construct operators which when measured in pairs can exhibit correlations, between the measurement outcomes of the two operators, which are stronger than what is permitted by NCHVMs.

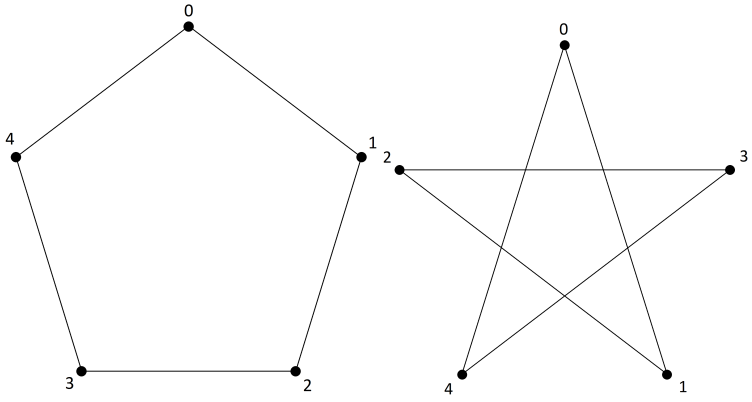

Figure 6.1: To the left we have a pentagon and to the right a pentagram. The two graphs represents the same relation between vertices as can be seen by the labeling.

[1]What they actually use is the pentagram graph. However the pentagram and the pentagon are equivalent, just relabel the vertices from {0,1,2,3,4} to {0,3,1,4,2} for instance.

6.2 Derivation

As was stated in the last section the operators used in this test are derived from the pentagon graph. This is done by taking an orthogonal representation of the graph and letting the projectors specified by these vectors represent the negative valued eigenstates of the operators we are looking for. The positive valued eigenstates are defined by any two orthogonal vectors lying in the plane orthogonal to the first vector. We have five vectors; $|v_0\rangle$, $|v_1\rangle$, $|v_2\rangle$, $|v_3\rangle$, and $|v_4\rangle$ related by $\langle v_i|v_{i+1}\rangle = 0$, that define five projectors; $Q_i = |v_i\rangle\langle v_i|$.

If we assume the world can be described by a NCHVT, and we want to calculate the sum of the expectation values of the projectors Q_i, lets denote it by W, we can easily see that it has to be less or equal to two. Say for instance that the system projects on Q_1, this means that it cannot project on Q_0 or Q_2, and similarly it can only project on one of Q_3 and Q_4[1]. Thus $W = \sum_{i=0}^{4} < Q_i > \leq 2$.

Now lets construct the operators $A_i \equiv 2Q_i - \mathbb{1}$, and look at the correlations. More specifically consider

$$K \equiv < A_0A_1 > + < A_1A_2 > + < A_2A_3 > + < A_3A_4 > + < A_4A_0 > .$$

By the definition of A_i we have that,

$$\begin{aligned} A_iA_{i+1} =& (2\,|v_i\rangle\langle v_i| - \mathbb{1})(2\,|v_{i+1}\rangle\langle v_{i+1}| - \mathbb{1}) \\ =& 4\,|v_i\rangle\langle v_i|v_{i+1}\rangle\langle v_{i+1}| - 2\,|v_i\rangle\langle v_i| - 2\,|v_{i+1}\rangle\langle v_{i+1}| + \mathbb{1}, \end{aligned}$$

but $\langle v_i|v_{i+1}\rangle = 0$ and all operators appear exactly twice in K so

$$K = < 5 \cdot \mathbb{1} - 4 \sum_{i=0}^{4} |v_i\rangle\langle v_i| > .$$

We have that $\sum_{i=0}^{4} < |v_i\rangle\langle v_i| > = \sum_{i=0}^{4} < Q_i > = W \leq 2$ which finally gives us

$$K = 5 - 4 \cdot W \geq -3.$$

This can easily be visualized by letting $a_i = \pm 1$ be the values that A_i can take, and then try to minimize the value of $K = a_0a_1 + a_1a_2 + a_2a_3 + a_3a_4 + a_4a_0$. Now $a_ia_{i+1} = -1$ if a_i and a_{i+1} have different signs, so minimizing K we can set $a_0 = 1$, $a_1 = -1$, $a_2 = 1$, and $a_3 = -1$, this sums the first three terms to -3, but when assigning a value to a_4 no matter how we choose, one of the two remaining terms will be 1 and the other -1, adding nothing to the total sum.

[1] This follows from the Kochen-Specker rules described in 5.1.

This is the bound for NCHVTs. If we consider quantum mechanical operators we should instead of W insert the Lovász number for the pentagon, which is $\sqrt{5}$ and we get $K \geq 5 - 4\sqrt{5} \approx -3.944$. This value is reached using the state:

$$|\psi\rangle = \begin{pmatrix} 0 \\ 0 \\ 1 \end{pmatrix},$$

and the operators defined by the states:

$$|v_0\rangle = \frac{1}{\sqrt{1+r^2}} \begin{pmatrix} 1 \\ 0 \\ r \end{pmatrix}, |v_1\rangle = \frac{1}{\sqrt{1+r^2}} \begin{pmatrix} \cos\frac{4\pi}{5} \\ \sin\frac{4\pi}{5} \\ r \end{pmatrix}, |v_2\rangle = \frac{1}{\sqrt{1+r^2}} \begin{pmatrix} \cos\frac{2\pi}{5} \\ -\sin\frac{2\pi}{5} \\ r \end{pmatrix},$$

$$|v_3\rangle = \frac{1}{\sqrt{1+r^2}} \begin{pmatrix} \cos\frac{2\pi}{5} \\ \sin\frac{2\pi}{5} \\ r \end{pmatrix}, |v_4\rangle = \frac{1}{\sqrt{1+r^2}} \begin{pmatrix} \cos\frac{4\pi}{5} \\ -\sin\frac{4\pi}{5} \\ r \end{pmatrix}.$$

6.3 Setup

The setup for the KCBS experiment is both an extension, and a simplificaton of the setups for the dimension witnesses since we will be measuring two operators sequentially but are only concerned with qutrit states, see Fig. (6.2).

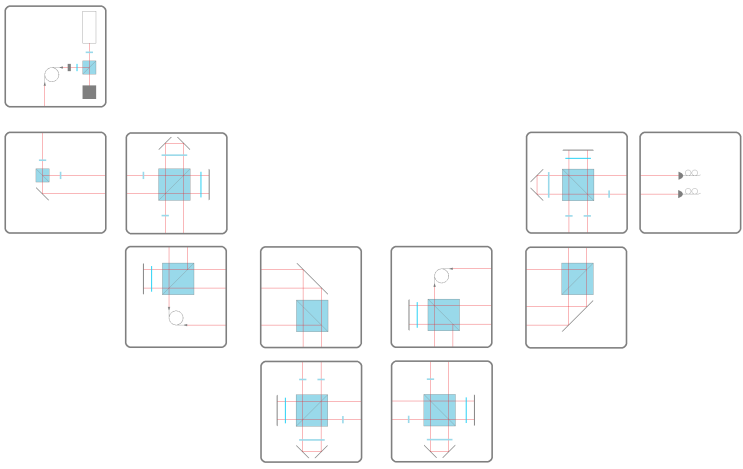

Figure 6.2: The setup for the KCBS-experiment.

The P-box

The difference in the P-box (see Fig. (6.3)) in the KCBS and Wright experiments as compared to the dimension witness experiments is the single photon source. In these experiments instead of using a continous wave laser we used a pulsed laser which gave us 100 000 pulses, with 3ns duration, every second. This enabled us to encode measurement results in time. There is also a difference in the state preparation part (see Fig. (6.4)), since we in this experiment only use qutrits we do not wish to have a HWP in the b mode.

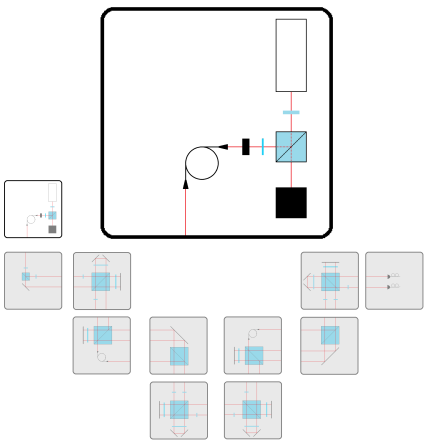

Figure 6.3: The source of emulated single photons. Directly after the laser we have a HWP to regulate the fraction reflected in the PBS (this works as a variable attenuator). Before the OD-filter we have a QWP so that any reflections from the filter or the fiber coupler will be turned to horizontal polarization and thus transmitted by the PBS. The optical fiber goes through a passive polarization controller so that we can set the polarization as we want it. This setup gives us nearly single photons in a single spatial mode and a set polarization mode.

The U-box

As before all measurements are dichotomic, and the two outcomes for each measurement is determined by the sign of the eigenvalues. The U-box has the same basic structure as for the optimal dimension witness, see Fig. (6.5); a HWP in mode a, a twisted polarizing Michelson interferometer to move the vertical component in the a mode to the b mode and flipping the polarizations, and a HWP in the b mode. But in this experiment we have interchanged which eigenstates go where, resulting in:

$$\begin{aligned} |+\rangle &\equiv |H,b\rangle \\ |-\rangle &\equiv \alpha\,|V,a\rangle + \beta\,|V,b\rangle. \end{aligned} \tag{6.1}$$

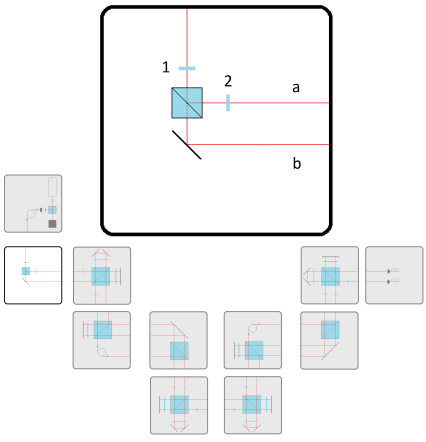

Figure 6.4: State preparation. A HWP turns the polarizations so that we can distribute the photon state over our two spatial modes. There is a HWP in mode a in order to distribute the photon state over the polarization modes.

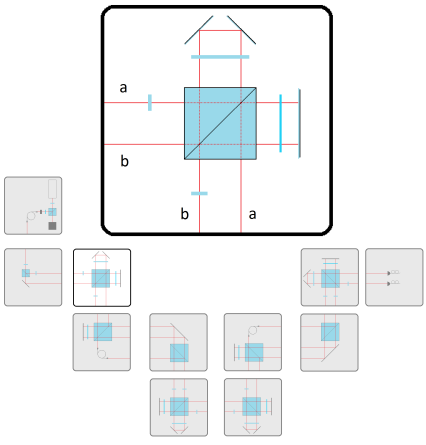

Figure 6.5: Unitary transformation from laboratory basis to eigenbasis of the operator. The first HWP interferes the polarization modes in mode a. The polarizing Michelson interferometer transfere the $|V,a\rangle$-component to $|H,b\rangle$, $|H,a\rangle$ to $|V,a\rangle$, and $|H,b\rangle$ to $|V,b\rangle$. Finally, the second HWP interferes the polarization modes in mode b.

The E-box

As seen above the U-box rotates the state so that the positive-valued eigenstate of the observable will be $|m_i\rangle = |H,b\rangle$. As can be seen in Fig. (6.6) a PBS placed over both spatial modes will split off the $|H,b\rangle$-part of the state and direct it into a short optical fiber. All polarizations are once more flipped and a PBS is used to reintroduce the, now delayed by Δt, $|V,b\rangle$-part (see Fig. (6.7)). The E-box has now entangled the negative-valued eigenstates with the time delays τ_{Y0} [1] and the positive-valued eigenstate with time delays τ_{Y1}.

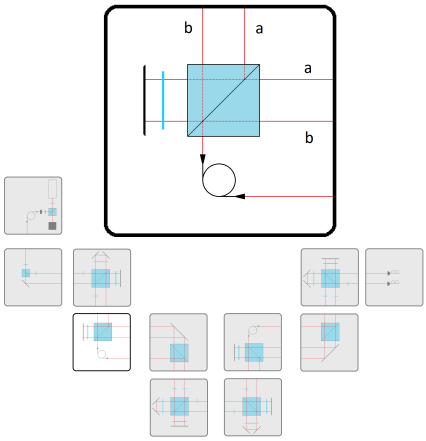

Figure 6.6: Entangling eigenstates of different eigenvalue with different degrees of freedom. The PBS splits the $|H,b\rangle$-component from the $|V,b\rangle$-component and transmits it into a single mode fiber. The fiber flips the polarization of the $|H,b\rangle$-component and introduces a time delay between different valued eigenstates. The polarization of the $|V,a\rangle$- and $|V,b\rangle$-component is flipped by the QWP and the mirror.

The U†-box

The transformation back to the laboratory basis is the reverse of the transformation done by the U-box. First the polarisation needs to be flipped, this is done by HWPs in each spatial mode, then a twisted polarizing Michelson interferometer moves the interchanged parts back, and finally a HWP in mode a undoes the initial rotation of the polarization modes, see Fig. (6.8).

[1]The index of τ is a binary number indicating the amount of time delay, in units of Δt, which is introduced to the state.

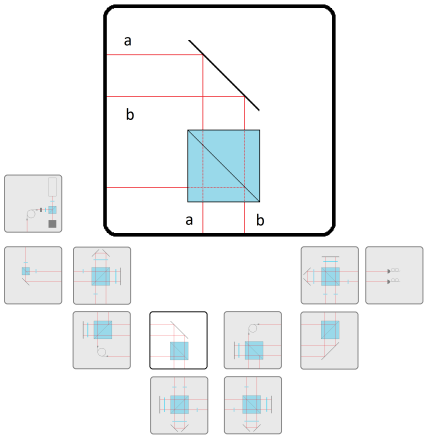

Figure 6.7: Reintroducing the delayed eigenstate to the system. Since the positive valued eigenstate is vertically polarized and the negative valued ones are horizontally polarized, a PBS can be used to reintroduce the positive valued eigenstate into mode b.

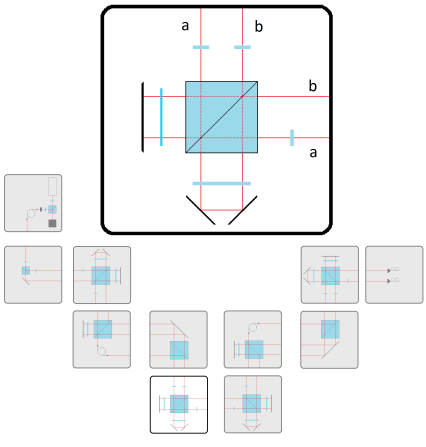

Figure 6.8: Unitary transformation from eigenbasis of the operator to the laboratory basis. The HWP in mode a flips the polarization from H to V and the HWP in mode b will undo the second interference from the U-box. The polarizing Michelson interferometer will transfere the $|V,a\rangle$-component to $|H,a\rangle$, $|H,b\rangle$ to $|V,a\rangle$, and $|V,b\rangle$ to $|H,b\rangle$. Finally the HWP in mode a will undo the first interference from the U-box.

The second operator

At this stage the photonic state enters another U-box which is constructed in the same way as the first one, but with different settings of the HWPs. The state then goes to the second E-box, which entangles the negative-valued eigenstates with the time delays τ_{0X} and the positive-valued eigenstate with time delays τ_{1X}. After which the photonic state is once again rotated back to the laboratory basis.

The D-box

The D-box consists of APDs in the output modes of the $U^{\dagger}$-box and a coincidence counter which, with the help of a pulse generator, determines at which time delay (τ_{00}, τ_{01}, τ_{10} or τ_{11}) the photon is detected.

6.4 Results

According to the KCBS-inequality NCHVTs predict that the sum of the expectation values of five dichotomic observables, is always greater than -3, if neighboring observables are exclusive. If we instead consider quantum mechanical observables, the bound is moved to $5-4\sqrt{5} \approx -3.944$. Our experimental results are presented in table (6.1), the two orders of the operators are presented on either side of the theoretical values. It is worth noteing that the results seem to indicate that the order of the observables does matter, however we would like to claim that this is an artefact due to the alignment process.

Table 6.1: Experimental results for the violation of the KCBS-inequality. The two main sources of error are given in the outermost columns from each side, the poissonian counting error and the systematic error. **The colored columns are again of most interest with the total error, the experimentally measured expectation values, and the theoretical values in the middle. Each side represents different order of the operators**.

i	$\Delta_{poisson}$	Δ_{syst}	Δ_{tot}	$\langle P_i P_{i+1} \rangle$	Theory	$\langle P_{i+1} P_i \rangle$	Δ_{tot}	Δ_{syst}	$\Delta_{poisson}$
0	0.002	0.023	0.023	-0.712	-0.789	-0.785	0.022	0.022	0.003
1	0.002	0.023	0.023	-0.706	-0.789	-0.781	0.023	0.023	0.003
2	0.002	0.022	0.022	-0.704	-0.789	-0.774	0.023	0.023	0.003
3	0.002	0.022	0.022	-0.708	-0.789	-0.774	0.022	0.022	0.003
4	0.002	0.024	0.024	-0.706	-0.789	-0.782	0.021	0.021	0.003
Σ	0.115	0.005	0.11	-3.5	-3.944	-3.9	0.11	0.115	0.006

7. Wright

The Wright inequality[17] is the simplest inequality where quantum mechanics violates the classical bound. It is simplest in the sense that you cannot get a quantum violation of the classical maximum with fewer measurements or a state with smaller dimension. This chapter is based on one of the experiments described in Paper III.

7.1 Theory

The easiest way to give a setting for Wright's inequality is by introducing a game of boxes and coins. Let the number of boxes be five and place them in a circle, start the game by placing a coin in one of the boxes. Now one box is choosen at random, this box and the one two steps in the clockwise direction is opened. Let the probability of finding the coin given the choice of a certain box, B_i, be denoted $P(+1|B_i)$ and construct the function:

$$W \equiv \sum_{i=0}^{4} P(+1|B_i). \tag{7.1}$$

In any given round of the game two choices of boxes have the potential of uncovering the coin[1], resulting in $W = 2$.

If we assign to each box B_i, a vector v_i and define the orthogonality relation by the possibility of uncovering the coin, i.e, $\langle v_i|v_{i+1}\rangle = 0$, we see that again we have the pentagon graph and we know that the independence number is 2. We can also make the observation that $P(+1|B_i) =< |v_i\rangle\langle v_i| >= |\langle v_i|\psi\rangle|^2$, and thus W is the Lovász number of the pentagon, which is $\sqrt{5}$. This value is reached using the projectors defined by the vectors found for the KCBS inequality:

$$|v_0\rangle = \frac{1}{\sqrt{1+r^2}}\begin{pmatrix}1\\0\\r\end{pmatrix}, |v_1\rangle = \frac{1}{\sqrt{1+r^2}}\begin{pmatrix}\cos\frac{4\pi}{5}\\ \sin\frac{4\pi}{5}\\ r\end{pmatrix}, |v_2\rangle = \frac{1}{\sqrt{1+r^2}}\begin{pmatrix}\cos\frac{2\pi}{5}\\ -\sin\frac{2\pi}{5}\\ r\end{pmatrix},$$

$$|v_3\rangle = \frac{1}{\sqrt{1+r^2}}\begin{pmatrix}\cos\frac{2\pi}{5}\\ \sin\frac{2\pi}{5}\\ r\end{pmatrix}, |v_4\rangle = \frac{1}{\sqrt{1+r^2}}\begin{pmatrix}\cos\frac{4\pi}{5}\\ -\sin\frac{4\pi}{5}\\ r\end{pmatrix},$$

and the test state:

$$|\psi\rangle = \begin{pmatrix}0\\0\\1\end{pmatrix}.$$

[1]Namely if we choose the box with the coin inside or the box two steps in the counterclockwise direction of the one with the coin inside.

7.2 Setup

The setup for the Wright experiment is the setup for the first operator of the KCBS-inequality, see Fig. (7.1). We could have done this experiment without transforming back to the laboratory basis, but since the setup was part of the larger KCBS-setup it was easier to use the same detection scheme.

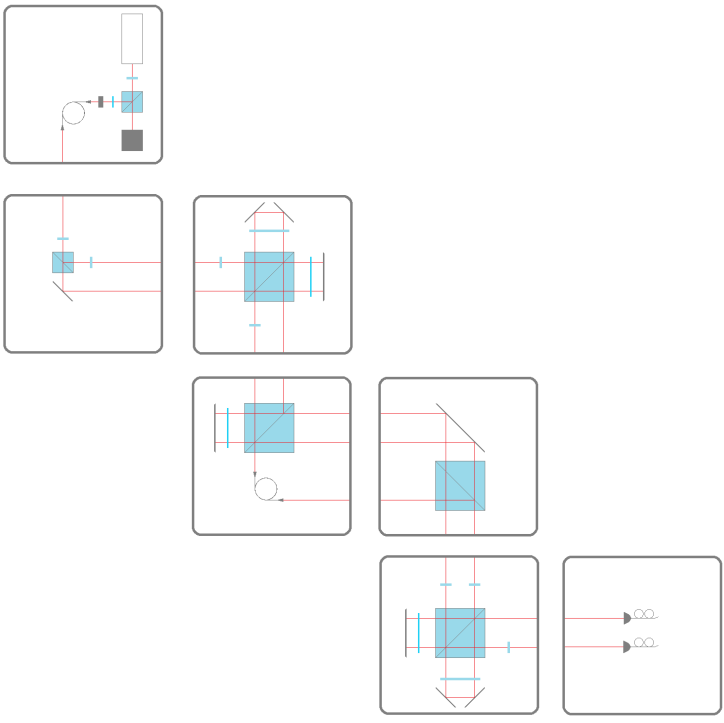

Figure 7.1: The setup for the wright experiment.

The P-box

The difference in the P-box (see Fig. (7.2)) in the Wright and Klyachko experiments as compared to the dimension witness experiments is the single photon source. In these experiments instead of using a continous wave laser we used a pulsed laser which gave us 100 000 pulses, with 3ns duration, every second. This enabled us to encode measurement results in time. There is also a difference in the state preparation part (see Fig. (7.3)), since we in this experiment only use qutrits we do not wish to have a HWP in the b mode.

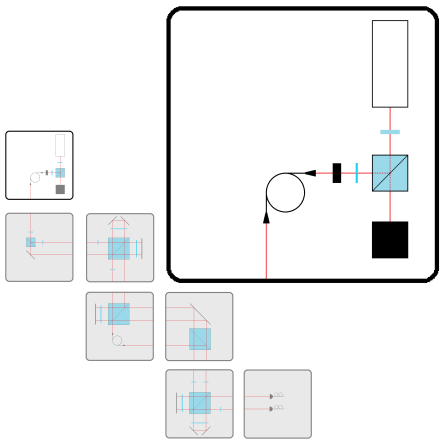

Figure 7.2: The source of emulated single photons. Directly after the laser we have a HWP to regulate the fraction reflected in the PBS (this works as a variable attenuator). Before the OD-filter we have a QWP so that any reflections from the filter or the fiber coupler will be turned to horizontal polarization and thus transmitted by the PBS. The optical fiber goes through a passive polarization controller so that we can set the polarization as we want it. This setup gives us nearly single photons in a single spatial mode and a set polarization mode.

The U-box

As before all measurements are dichotomic, and the two outcomes for each measurement is determined by the sign of the eigenvalues. The U-box has the same basic structure as for the optimal dimension witness, see Fig. (7.4); a HWP in mode a, a twisted polarizing Michelson interferometer to interchange the vertical components and flipping the polarizations, and a HWP in the b mode. But in this experiment we have interchanged which eigenstates go where, resulting in:

$$\begin{aligned} |+\rangle &\equiv |H,b\rangle \\ |-\rangle &\equiv \alpha\,|V,a\rangle + \beta\,|V,b\rangle. \end{aligned} \tag{7.2}$$

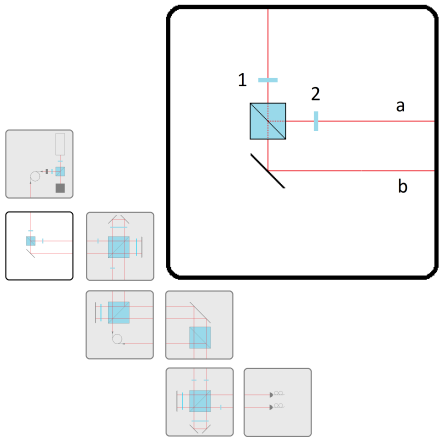

Figure 7.3: The preparations of quantum states. A HWP turns the polarizations so that we can distribute the photon state over our two spatial modes. There is a HWP in mode a in order to distribute the photon state over the polarization modes.

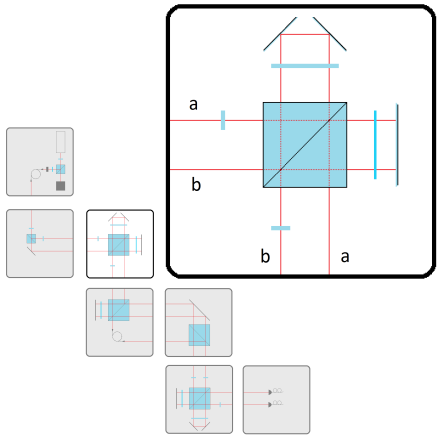

Figure 7.4: Unitary transformation from laboratory basis to eigenbasis of the operator. The first HWP interferes the polarization modes in mode a. The polarizing Michelson interferometer transfere the $|V,a\rangle$-component to $|H,b\rangle$, $|H,a\rangle$ to $|V,a\rangle$, and $|H,b\rangle$ to $|V,b\rangle$. Finally, the second HWP interferes the polarization modes in mode b.

The E-box

As seen above the U-box rotates the state so that the positive-valued eigenstate of the observable will be $|m_i\rangle = |H,b\rangle$. As can be seen in Fig. (7.5) a PBS placed over both spatial modes will split off the $|H,b\rangle$-part of the state and direct it into a short optical fiber. All polarisations are once more flipped and a PBS is used to reintroduce the, now slightly delayed, $|V,b\rangle$-part (see Fig. (7.6)). The E-box has now entangled the negative-valued eigenstates with the time τ_0 and the positive-valued eigenstate with time τ_1.

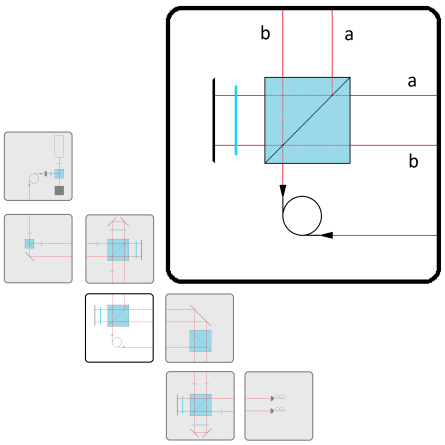

Figure 7.5: Entangling eigenstates of different eigenvalue with different degrees of freedom. The PBS splits the $|H,b\rangle$-component from the $|V,b\rangle$-component and transmits it into a single mode fiber. The fiber flips the polarization of the $|H,b\rangle$-component and introduces a time delay between different valued eigenstates. The polarization of the $|V,a\rangle$- and $|V,b\rangle$-component is flipped by the QWP and the mirror.

The $U^{\dagger}$-box

There is not really a need of a $U^{\dagger}$-box since we will only make single measurements and detection directly after the E-box would be sufficient. This setup was part of the Klyachko setup however, and in that setup we needed to get back to the laboratory basis. The transformation back is the reverse of the transformation done by the U-box. First the polarisation needs to be flipped, this is done by HWPs in each spatial mode, then a twisted polarizing Michelson interferometer moves the interchanged parts back, and finally a HWP in mode a undoes the initial rotation of the polarization modes, see Fig. (7.7).

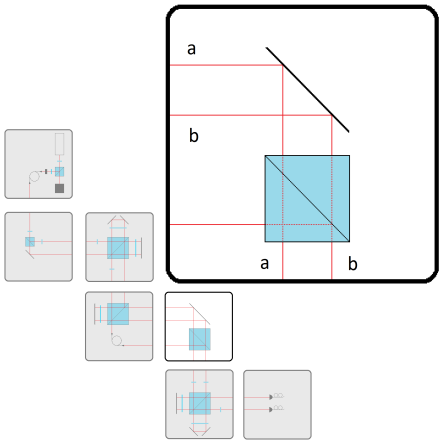

Figure 7.6: Reintroducing the delayed eigenstate to the system. Since the positive valued eigenstate is vertically polarized and the negative valued ones are horizontally polarized, a PBS can be used to reintroduce the positive valued eigenstate into mode b.

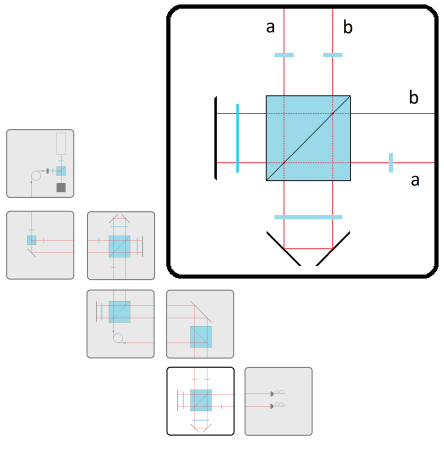

Figure 7.7: Unitary transformation from eigenbasis of the operator to the laboratory basis. The HWP in mode a flips the polarization from H to V and the HWP in mode b will undo the second interference from the U-box. The polarizing Michelson interferometer will transfere the $|V,a\rangle$-component to $|H,a\rangle$, $|H,b\rangle$ to $|V,a\rangle$, and $|V,b\rangle$ to $|H,b\rangle$. Finally the HWP in mode a will undo the first interference from the U-box.

The D-box

The D-box consists of APDs in the output modes of the $U^{\dagger}$-box and a coincidence counter which, with the help of a pulse generator, determines at which time (τ_0 or τ_1) the photon is detected.

7.3 Results

Assume that we have a set of five statements, where each statement is exclusive to two other. Then the Wright inequality states that if we sum the probabilities, that each statement is true, we will get a value which is less than or equal to 2. If this is set in a quantum mechanical setting the sum of the probabilities can reach $\sqrt{5} \approx 2.24$.Our experimental results from the Wright inequality test are presented in table (7.1).

Table 7.1: Experimental results for the violation of Wright's inequality. The columns specify the theoretical values, the experimentally measured values, the systematic errors, the poissonian counting errors, and the total errors. **The colored columns are of most interest and show the theoretical values, the experimentally measured values, and the total experimental error, respectively**.

Projector	$P(+1\|P_i)_{Th}$	$P(+1\|P_i)_{Exp}$	Δ_{syst}	$\Delta_{poisson}$	Δ_{tot}
0	0.447	0.4600	0.0112	0.0012	0.0113
1	0.447	0.4544	0.0112	0.0012	0.0113
2	0.447	0.4603	0.0112	0.0016	0.0113
3	0.447	0.4610	0.0112	0.0011	0.0112
4	0.447	0.4566	0.0112	0.0010	0.0112
Σ	2.236	2.29	0.0559	0.03	0.06

8. Hardy

This chapter will describe an experiment that shows a direct conflict between quantum mechanics and NCHVTs in the sense that quantum mechanics gives a non-zero probability for an event that cannot occur according to NCHVTs. Lucien Hardy wrote two papers in the 1990's[18; 19] where he outlines an experiment which would give this kind of contradiction for entangled qubits. These experiments inspired the writing of a paper by Cabello, Badziąg, Cunha, and Bourennane in the summer of 2013[20]. This chapter is based on the experiment described in Paper IV.

8.1 Motivation

The idea behind this experiment is that a "Hardy argument" for non-contextual inequalities would in some sense be the cleanest violation of NCHVT. So to start with, lets refresh what Hardy's argument was.

The first idea that Hardy had was to make a similar statement as Greenberger, Horne, and Zeilinger[21] had done for three particles, but for a system of only two particles. Even though this is possible if we consider a situation where the number of settings of the local measurements are infinite, it is impossible to use the same procedure for a finite set of measurements. Instead, consider the situation where we have two boxes, A and B, with two buttons each, labeled $\{a_1, a_2\}$ and $\{b_1, b_2\}$ respectively. Let us now send one particle to each box in a state such that we get the measurement probabilities:

$$\begin{aligned} P(1,1|a_1,b_2) &= 0 \\ P(1,1|a_2,b_1) &= 0 \\ P(0,0|a_2,b_2) &= 0, \end{aligned}$$

where $P(\alpha,\beta|a_i,b_j)$ is the probability to get the measurement outcomes α and β when box A is set to a_i and box B to b_j. A HVT would predict that $P(1,1|a_1,b_1) = 0$ by necessity, however with an entangled state and suitable measurement settings we can get $P(1,1|a_1,b_1) = \frac{1}{16}$.

8.2 Derivation

As we saw in the last section, it is possible to transform the CHSH-inequality to a direct contradiction between LHVTs and experiment outcomes. In this chapter we will do a similar thing to the KCBS-inequality.

In chapter 6 we saw that we could describe the classical bound of the KCBS-inequality with a game of five boxes and one coin. In the spirit of Hardy's argument we now want to find restrictions on the probabilities to uncover the coin so that we get a contradiction for some measurement outcome.

If we have the five choices of pairs P_1, P_2, P_3, P_4, and P_5, then let A be the set of preparations for which P_1 uncover the coin, and B, the set for P_2, C for P_3, D for P_4, and E for P_5. Also let A^c be the compliment of A, i.e, the set of preparations for which P_1 do not uncover the coin, and likewise for B^c, C^c, D^c, and E^c. Now we make the restrictions:

$$\mathrm{P}(\mathrm{A}^c \cap \mathrm{B}) + \mathrm{P}(\mathrm{B}^c \cap \mathrm{C}) = 1 \tag{8.1}$$

$$\mathrm{P}(\mathrm{C}^c \cap \mathrm{D}) + \mathrm{P}(\mathrm{D}^c \cap \mathrm{E}) = 1, \tag{8.2}$$

which makes a NCHVT predict that $\mathrm{P}(\mathrm{E}^c \cap \mathrm{A}) = 0$. This is easy to see since from equation 8.1 we have that $\mathrm{A} \subseteq \mathrm{C}$ and from 8.2 that $\mathrm{C} \subseteq \mathrm{E}$, thus $\mathrm{A} \subseteq \mathrm{E}$, and obviously $\mathrm{P}(\mathrm{E}^c \cap \mathrm{E}) = 0$.

In order to test this prediction in the lab we need to find observables, that can correspond to opening boxes looking for the coin, and a test state, that can correspond to the distribution of the coin. We design observables of the form: $O_i = 2\,|v_i\rangle\langle v_i| - \mathbb{1}$, and make the identification that the preparations in the classical game correspond to the positive eigenstates of our observables: $\mathrm{A} \Rightarrow |v_1\rangle\langle v_1|$, $\mathrm{B} \Rightarrow |v_2\rangle\langle v_2|$, $\mathrm{C} \Rightarrow |v_3\rangle\langle v_3|$, $\mathrm{D} \Rightarrow |v_4\rangle\langle v_4|$, and $\mathrm{E} \Rightarrow |v_5\rangle\langle v_5|$. This means that we can write, for instance $\mathrm{P}(\mathrm{E}^c \cap \mathrm{A})$ as $\mathrm{P}(O_5 = -1, O_1 = 1)$ or $\mathrm{P}(-1,1|O_5,O_1)$ as a more convenient notation and thus we can write equations 8.1 and 8.2 as:

$$\mathrm{P}(-1,1|O_1,O_2) + \mathrm{P}(-1,1|O_2,O_3) = 1 \tag{8.3}$$

$$\mathrm{P}(-1,1|O_3,O_4) + \mathrm{P}(-1,1|O_4,O_5) = 1. \tag{8.4}$$

The restriction that "neighbouring" pairs have no common boxes in the classical game corresponds to that "neighbouring" eigenstates, $|v_i\rangle$ and $|v_{i+1}\rangle$, are orthogonal. These conditions can be used in the maximization of the probability $\mathrm{P}(-1,1|O_5,O_1)$ to find the optimal test state:

$$|\eta\rangle = \frac{1}{\sqrt{3}} \begin{pmatrix} 1 \\ 1 \\ 1 \end{pmatrix}, \tag{8.5}$$

and eigenstates for the operators:

$$|v_1\rangle = \frac{1}{\sqrt{3}}\begin{pmatrix}1\\-1\\1\end{pmatrix}, |v_2\rangle = \frac{1}{\sqrt{2}}\begin{pmatrix}1\\1\\0\end{pmatrix}, |v_3\rangle = \begin{pmatrix}0\\0\\1\end{pmatrix},$$
$$|v_4\rangle = \begin{pmatrix}1\\0\\0\end{pmatrix}, |v_5\rangle = \frac{1}{\sqrt{2}}\begin{pmatrix}0\\1\\1\end{pmatrix}. \tag{8.6}$$

These choices yields the probability $\mathrm{P}(-1,1|O_5,O_1) = \frac{1}{9}$, which is in clear contradiction to the prediction of NCHVTs.

8.3 First setup

The first setup that was built for this experiment was based on the idea that only certain projection combinations were needed. As we have seen we have two conditions for our system:

$$\begin{aligned} \mathrm{P}(\mathrm{A}^c \cap \mathrm{B}) + \mathrm{P}(\mathrm{B}^c \cap \mathrm{C}) &= 1 \\ \mathrm{P}(\mathrm{C}^c \cap \mathrm{D}) + \mathrm{P}(\mathrm{D}^c \cap \mathrm{E}) &= 1. \end{aligned} \tag{8.7}$$

These conditions could be interpreted as:

$$\begin{aligned} \mathrm{P}(\mathrm{A}^c|\mathrm{B}) + \mathrm{P}(\mathrm{C}|\mathrm{B}^c) &= 1 \\ \mathrm{P}(\mathrm{C}^c|\mathrm{D}) + \mathrm{P}(\mathrm{E}|\mathrm{D}^c) &= 1 \end{aligned} \tag{8.8}$$

which can be seen as restrictions on chains of events ending in the outcome probabilities; $\mathrm{P}(\mathrm{A}|\mathrm{B})$, $\mathrm{P}(\mathrm{A}^c|\mathrm{B})$, $\mathrm{P}(\mathrm{C}|\mathrm{B}^c)$, and $\mathrm{P}(\mathrm{C}^c|\mathrm{B}^c)$ for the first and $\mathrm{P}(\mathrm{C}|\mathrm{D})$, $\mathrm{P}(\mathrm{C}^c|\mathrm{D})$, $\mathrm{P}(\mathrm{E}|\mathrm{D}^c)$, and $\mathrm{P}(\mathrm{E}^c|\mathrm{D}^c)$ for the second.

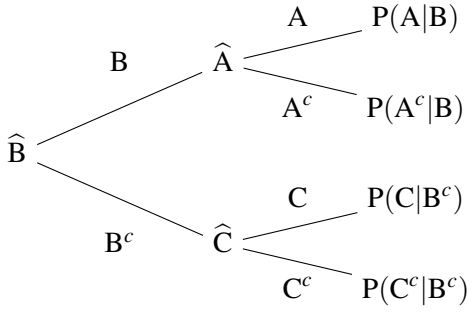

This would seem to implicate that if we implement observable $\widehat{\mathrm{B}}$, we could implement both $\widehat{\mathrm{A}}$ and $\widehat{\mathrm{C}}$ at the same time by letting the positive valued eigenstate of $\widehat{\mathrm{B}}$ go to $\widehat{\mathrm{A}}$ and the negative valued eigenstates go to $\widehat{\mathrm{C}}$. While this is sufficient in an ideal scenario the additional outcome probabilities that we can measure if we let the whole state propagate through both $\widehat{\mathrm{A}} \cdot \widehat{\mathrm{B}}$ and $\widehat{\mathrm{C}} \cdot \widehat{\mathrm{B}}$ can provide us with information which will be of great interest. For instance the probability $\mathrm{P}(\mathrm{C} \cap \mathrm{B})$ can be seen as a measure of the compatibility of $\widehat{\mathrm{C}}$ and $\widehat{\mathrm{B}}$, and the probability $\mathrm{P}(\mathrm{A}^c \cap \mathrm{B}^c)$ can be seen as a measure of how well the probe state $|\eta\rangle$ is prepared with respect to $\widehat{\mathrm{A}}$ and $\widehat{\mathrm{B}}$.

Since the first idea was that just the special sequences needed to be measured, the first setup was constructed accordingly.

The P-box

The state needed to test this contradiction is a qutrit with equal weight in all levels which are all in phase. For this experiment we have chosen to use three spatial modes to encode our qutrits in. To create a state like this we need a

single photon source and then be able to split the probability amplitude into the three levels. This is easily done with two HWPs and two PBS's, however this will result in the three modes having different polarization so we need one more HWP to adjust the polarization in the differing mode.

The U-boxes

Since we are only using spatial modes for encoding in this experiment the transformations are not as simple as in previous experiments. So instead of implementing a general unitary transformation, each observable is implemented individualy. The five observables are defined by the projectors onto the states (8.6).

- The first observable consists of a phase-plate in mode b to introduce a π phase shift, then a 50:50 BS to interfere mode b and c, and finally a 33:67 BS to interfere mode a and b.
- The second observable consists of a 50:50 BS to interfere mode a and b.
- The third observable consists of just permuting mode a to b, b to c, and c to a.
- The fourth observable is the identity, i.e., it does nothing.
- The fifth obsevable consists of a 50:50 BS to interfere mode b and c, and transposing a and b.

The E-box

The entangling in this setup is very simple, mode a is representing the positive valued eigenstate and is directed in one direction while mode b and c represents the negative valued eigenstates and are directed in another direction.

The $U^{\dagger}$-boxes

When implementing the transformation back to the laboratory basis we just need to reverse the actions taken in the corresponding U-box. This is only needed for the first observable in the sequence since the E-box following the second transformation has made all the possible outcomes for the experiment distinguishable.

The D-box

The detection is done by an APD in each output mode of the second E-box.

8.4 Final setup

To accomodate for the probabilities that were left out in the first setup, the experiment needed to be expanded to include all possible projection combinations. This work was done by Breno Marques[1]. In this setup we made the decision to encode the outcome of the first operator in polarization and then have detection directly after the second E-box, which separates the eigenstates into different spatial modes.

[1] When the new setups were designed both of us checked that the operators of the two experiments were the same.

8.5 Results

The idea that Hardy had to create a conflict between LHVTs and quantum mechanics resulted in an outcome probability of $\frac{1}{16}$ for an entangled pair, of an event with zero probability according to LHVTs. When adjusted to the KCBS-inequality we get an outcome probability of $\frac{1}{9}$, for an event that according to NCHVTs cannot happen.

Table 8.1: Experimental results for the final setup of the Hardy experiment. The index to the left indicates which pair of operators have been measured. The experimental data is given in the two columns to the right, measured in the order indicated by the indecies.

i	Theory	$P(0,1\|i,i+1)$	$P(0,1\|i+1,i)$
1	0.667	0.635 ± 0.020	0.661 ± 0.011
2	0.333	0.332 ± 0.008	0.331 ± 0.005
3	0.333	0.330 ± 0.004	0.339 ± 0.003
4	0.667	0.650 ± 0.008	0.656 ± 0.011
5	0.111	0.111 ± 0.003	0.109 ± 0.004

9. Further discussions on noncontextuality

In this thesis we have discussed experimental implementations of dimension witnesses and non-contextual inequalities. As a conclusion of the thesis I will end by reviewing some problems and topics regarding noncontextuality that are only loosely connected to the work presented in this thesis. Some issues were known before I started the experiments and some have evolved during the time of my studies. The work presented in this chapter has all been done by other people and/or groups.

9.1 State independent noncontextuality inequalities

The experimental violation of noncontextuality inequalities presented in this thesis are state dependent, i.e., for a given inequality we need to optimize the state in order to get the maximal violation[1]. However the beauty of the Kochen-Specker theorem is that it is state independent, i.e., it does not matter how you prepare your state, there will always be a violation if the world cannot be explained with NCHVT.

Cabello[22] conceived of an experiment based on nine observables ordered in three rows and three columns where the expectation value of each row and each column is equal to unity except for the last column which has expectation value equal to minus one. This is a system which is impossible to construct in a NCHVM and we can construct an inequality

$$\chi = \langle ABC \rangle + \langle abc \rangle + \langle \alpha\beta\gamma \rangle + \langle Aa\alpha \rangle + \langle Bb\beta \rangle - \langle Cc\gamma \rangle \leq 4 \tag{9.1}$$

which is violated to the maximum value 6 by any quantum state. This was done experimentally with linear optics by Amselem, Rådmark, Cabello, and Bourennane[23].

[1] As a matter of fact optimization is needed to get any violation at all.

9.2 Compatibility problems in noncontextuality

In experiments testing noncontextuality inequalities, a number of observables need to be implemented and measured sequentially in such a way that the measurement outcomes of all observables can be accessed. One of the demands is that the observables that are measured simultaneously are compatible. The fulfillment of this demand is hard to ensure since the implementation of the observables are susceptible to experimental errors. A way to assess the degree to which two observables are incompatible is to estimate the probability of the 'forbidden' outcome[1]. This probablity can then be taken as the fraction of the joint measurement for which the observables are incompatible and the bound of the inequality can be adjusted accordingly.

Another way to circumvent the problem of compatibility is to make use of entangled states[24]. This way the two observables will be operating on disjoint parts of the state[2].

[1]For two compatible observables there will be at least one eigenstate from each which is orthogonal to one of the eigenstates of the other. A simultaneous projection on these two eigenstates constitutes a forbidden measurement outcome.

[2]The observables are spacelike separated and operates only on the part of the state which is at the spatial location of the observable.

9.3 Context problems in noncontextuality

The group of Zeilinger in Vienna 'solved' the problem of compatibility for experiments with two successive observables by choosing a common basis for the implementation of the two observables[25]. This basis is one that simultaneously diagonalizes the observables. While this successfully ensures that the two observables are compatible it introduces a new problem, which is that an observable $\widehat{A}$ will be implemented differently depending on which other observable is measured simultaneously. This violates another demand which states that each observable needs to be the same no matter what context it is measured in. If this demand is not met a NCHVT can exploit this freedom and the inequality is no longer bounded by the theoretical bound. Another consequence of the way they implemented the observables is that they need to add an additional term to the inequality. They start their experiment with preparing a photonic state in three spatial modes. An operator acts on this state by projecting on three spatial modes[1], now another operator acts on the state by again projecting on three spatial modes[2]. They place detectors in two of the modes and the operators are designed in such a way that the eigenstate with eigenvalue -1 is projected on one of the modes terminated in a detector. For two successive operators a click in one of the two detectors corresponds to projection on the eigenstate with eigenvalue -1 of the corresponding operator.

[1] These three modes are now the eigenstates of the operator.

[2] Which are now the eigenstates of the second operator.

A. Components for experimental quantum optics

The following appendix is a direct citation from my Licentiate thesis.

All three experimental setups are built from the same optical components. They are even all part of the same setup, where the witness setup is made up of a general four-level operator. The Wright setup includes repreparation of the eigenstates in the same basis as the input state, and the Klyachko setup is expanded to two consecutive Wright setups. All setups can be divided into three parts, a state preparation part made up of a photon source, a beam splitter, and half-wave plates. This is followed by an operator part made up of a number of half-wave plates, beamsplitters, and optical fibers. Finally there is a detection part made up of optical fibers and single photon detectors. In addition there is an electronics layer for controlling the optics layer.

Laser

There were two different lasers used in the experiments; one was a pulsed diode laser with a wavelength of 780nm, it had a repetition rate of 100kHz and each pulse had a duration of 3ns. The other one was a continuous wave diode laser also centered at 780nm. Both lasers were attenuated until the number of coincidences were negligable. 1nm filters were used in order to increase the coherence length.

Wave plates

Birefringence is an effect that delays one polarization with respect to an orthogonal one. A zero order wave plate is a birefringent crystal cut so that this delay is within one wavelength of the light. Specifically there are two commonly used wave plates; quarter-wave and half-wave plates, these introduce a delay of precisely a quarter and half of a wavelength, respectively. By turning the waveplates in the plane perpendicular to the propagation direction of the light one can manipulate the polarization of the light.

A simple model of the action of a half-wave plate acting on linearly polarized light is to let a normal 2-D Cartesian coordinate system represent the

incoming polarization, now draw a line with the same inclination as the half-wave plate, mirror all points in this line and the resulting points are the outgoing polarization. Since elliptical polarization can be interpreted as a superposition of linear polarization this model can be expanded to include all polarization states.

Beam-splitters

There are different kinds of beam-splitters, in this thesis the polarizing beam-splitter (PBS) is the one used. The PBS transmit the horizontal part and reflect the vertical part of the light.

Single photon detectors

The detectors used in the experiments were of the avalanche-photo-diode (APD) type. They are used in a reverse bias mode (Geiger mode) so that when a photon is incident on the active area a charge carrier pair can be created, these will in turn collide with the lattice and create more pairs and so on building up an avalanche of charge carriers. This current is detected by the controlling electronics and upon detection a quenching circuit reduce the bias voltage so that the charge carriers are not accelerated, reducing the creation of additional pairs, letting the existing pairs dissipate.

The detectors produce TTL output signals of 4.1 Volt (with a duration of 41 ns). The dead time of the detectors is 50 ns. The detector signals were registered using a multi-channel coincidence logic with a coincidence time window of 1.7 ns. The coincidence time window was used to estimate multi-events and to define different time slots.

B. Error analysis

When doing experimental investigations it is crucial to understand what sources of error are present and how to take the effect of these errors in to account in the final result.

In the experiments presented in this thesis we have two main sources of error. These are the imperfections in the polarizing components[1] and the error due to the poissonian counting statistics caused by the fact that the detectors are not 100% efficient.

In order to assess the influence of the first error, models of the setups were made in Octave[2] where the imperfections could be inserted to see how they would affect the outcome. The transmission and reflectance of horizontal and vertical polarization in the PBSs were set to 99.5%[3] and the precision of the setting of the wave-plates were set to half a degree.

To assess how the detection error would affect the result the poisson error[4] was propagated through the expectation value calculation.

[1] In this error we include the imperfections of the physical object, i.e., nonperfect splitting by PBSs, as well as misalignment of wave-plates.

[2] Octave is a high-level interpreted language for numerical computations.

[3] This is the specification from the manifacturer.

[4] The poisson error is the square root of the detected events in one measurement bin, in our case the measurement bins were one second.

References

[1] A. EINSTEIN, B. PODOLSKY, AND N. ROSEN. **Can quantum-mechanical description of physical reality be considered complete?** *Phys. Rev.* ***47***, (1935). 12, 19

[2] S. FREEDMAN AND J. CLAUSER. **Experimental test of local hidden-variable theories.** *Phys. Rev. Lett.* ***28***, (1972). 12, 19

[3] S. KOCHEN AND E. P. SPECKER. **The problem of hidden variables in quantum mechanics.** *J. Math. Mech.* ***17,*** *59*, (1967). 12, 42

[4] H. BARTOSIK, J. KLEPP, C. SCHMITZER, S. SPONAR, A. CABELLO, H. RAUCH, AND Y. HASEGAWA. **Experimental test of quantum contextuality in neutron interferometry.** *Phys. Rev. Lett.* ***103***, (2009). 12

[5] J. S. BELL. **On the Einstein Podolsky Rosen paradox.** *Physics Vol.* ***1***, (1964). 19

[6] J. CLAUSER, M. HORNE, A. SHIMONY, AND R. HOLT. **Proposed experiment to test local hidden-variable theories.** *Phys. Rev. Lett.* ***23***, (1969). 19, 20, 23

[7] A. ASPECT, P. GRANGIER, AND G. ROGER. **Experimental test of realistic local theories via Bell's theorem.** *Phys. Rev. Lett.* ***47***, (1981). 19

[8] A. ASPECT, P. GRANGIER, AND G. ROGER. **Experimental realization of Einstein-Podolsky-Rosen-Bohm *Gedankenexperiment*: A new violation of Bell's inequalities.** *Phys. Rev. Lett.* ***49***, (1982).

[9] A. ASPECT, J. DALIBARD, AND G. ROGER. **Experimental test of Bell's inequalities using time-varying analyzers.** *Phys. Rev. Lett.* ***49***, (1982). 19

[10] J. S. BELL. **Discussion of experimental proof for the paradox of Einstein, Rosen, and Podolsky.** *Phys. Rev.* ***108***, (1957). 20

[11] A. CABELLO, S. SEVERINI, AND A. WINTER. **Graph-theoretic approach to quantum correlations.** *Phys. Rev. Lett.* ***112***, (2014). 21

[12] N. BRUNNER, S. PIRONIO, A. ACÍN, N. GISIN, A. MÉTHOT, AND V. SCARANI. **Testing the dimension of hilbert spaces.** *Phys. Rev. Lett.* ***100***, (2008). 24

[13] R. GALLEGO, N. BRUNNER, C. HADLEY, AND A. ACÍN. **Device-independent tests of classical and quantum dimensions.** *Phys. Rev. Lett.* ***105***, (2010). 24, 33

[14] H-W. LI, P. MIRONOWICZ, M. PAWŁOWSKI, Z-Q. YIN, Y-C. WU, S. WANG, W. CHEN, H-G. HU, G-C. GUO, AND Z-F. HAN. **Relationship between semi- and fully-device-independent protocols.** *Phys. Rev. A* ***87***, (2013). 24, 25

[15] C. BENNET AND G. BRASSARD. *Proc. IEEE International Conference on Computers, Systems, and Signal Processing, Bangalore, India . , p. 203*, (IEEE, 1984). 26

[16] A. A. KLYACHKO, M. A. CAN, S. BINICIOĞLU, AND A. S. SHUMOVSKY. **Simple test for hidden variables in spin-1 systems.** *Phys. Rev. Lett.* ***101***, (2008). 46

[17] R. WRIGHT. **The state of the pentagon.** *In Mathematical Foundations of Quantum Mechanics, edited by A. R. Marlow (Academic Press, San Diego), p. 255*, (1978). 57

[18] L. HARDY. **Quantum mechanics, local realistic theories, and Lorentz-invariant realistic theories.** *Phys. Rev. Lett.* ***68***, (1992). 67

[19] L. HARDY. **Nonlocality for two particles without inequalities for almost all entangled states.** *Phys. Rev. Lett.* ***71***, (1993). 67

[20] A. CABELLO, P. BADZIĄG, M. CUNHA, AND M. BOURENNANE. **Simple Hardy-like proof of quantum contextuality.** *Phys. Rev. Lett.* ***111***, (2013). 67

[21] D. GREENBERGER, M. HORNE, AND A. ZEILINGER. **Going beyond Bell's theorem.** In M. KAFATOS, editor, *Bell's theorem, quantum theory, and conceptions of the universe.* Kluwer, (1989). 68

[22] A. CABELLO. **Experimentally testable state-independent quantum contextuality.** *Phys. Rev. Lett.* ***101***, (2008). 76

[23] E. AMSELEM, M. RÅDMARK, M. BOURENNANE, AND A. CABELLO. **State-independent quantum contextuality with single photons.** *Phys. Rev. Lett.* ***103***, (2009). 76

[24] A. CABELLO, E. AMSELEM, K. BLANCHFIELD, M. BOURENNANE, AND I. BENGTSSON. **Proposed experiments of qutrit state-independent contextuality and two-qutrit contextuality-based nonlocality.** *Phys. Rev. A* ***85***, (2012). 77

[25] R. LAPKIEWICZ, P. LI, C. SCHAEFF, S. LANGFORD, N. RAMELÖW, M. WIEŚNIAK, AND A. ZEILINGER. **Experimental non-classicality of an indivisible quantum system.** *Nature* ***474***, (2011). 78

Part III

Papers